FACULTY OF BIOSCIENCE ENGINEERING

IMSOGLO INTERNATIONAL MASTER OF SCIENCE IN SOILS AND GLOBAL CHANGE

EFFECT OF SOIL ORGANIC MATTER QUALITY ON THE SOIL MOISTURE – HETEROTROPHIC RESPIRATION RELATIONSHIP

Xu Zhang

Student number: 02101998

Academic promotor: Prof. dr. Steven Sleutel

Master's Dissertation submitted to Ghent University in partial fulfilment of the requirements for the degree of International Master of Science in Soils and Global Change

Academic Year: 2022 - 2023

GHENT UNIVERSITY AARHUS UNIVERSITY GEORG-AUGUST-UNIVERSITÄT GÖTTINGEN BOKU

With the support of the Erasmus+ Programme of the European Union

COPYRIGHT

ACKNOWLEDGEMENTS

In composing this master thesis, I wish to extend my sincerest gratitude to prof. Steven Sleutel for his unwavering patience and invaluable hands-on guidance. His expertise and support have been instrumental in shaping the outcome of this work, and I am truly appreciative.

Additionally, I would like to acknowledge the considerable effort and resolute dedication I have channeled into this undertaking. The countless hours and steadfast commitment devoted to this thesis exemplify my aspiration to generate a substantial and meaningful contribution.

As I reflect upon this journey with IMSOGLO, it becomes evident that this expedition has been a profoundly enlightening odyssey. My heartfelt gratitude goes to all the exceptional teachers involved. Their provision of invaluable insights and creation of a rich learning environment have profoundly contributed to shaping my personal growth.

TABLE OF CONTENTS

Contents

LIST OF ABBREVIATIONS

C	Carbon
CO_2	Carbon dioxide
DOC	Dissolved organic carbon
DOM	Dissolved organic matter
GC	Gas Chromatography
GHGs	Greenhouse gases
IPCC	Intergovernmental Panel on Climate Change
MAOM	Mineral-associated organic matter
N	Nitrogen
NA	Missing data
NRMSE	Normalized root mean squared error
OM	Organic matter
POM	Particulate organic matter
R^2	R squared, coefficient of determination
Ra	Autotrophic respiration
Rh	Heterotrophic respiration
RMSE	Root mean squared error
Rs	Soil surface CO_2 flux
SIC	Soil inorganic carbon
SOC	Soil organic carbon
SOM	Soil organic matter
SWC	Volumetric soil water content
TOC	Total soil organic carbon
WFPS	Water-filled pore space level
WFPS%	Water-filled pore space percentage

LIST OF FIGURES

LIST OF TABLES

ABSTRACT

Understanding the dynamics of carbon mineralization in soil ecosystems is crucial for predicting carbon fluxes and mitigating climate change impacts. This study investigates the effects of soil moisture content on carbon mineralization through controlled laboratory experiments. We specifically wanted to see how the dependency of soil heterotrophic respiration (Rh) onto the % of water-filled pore space (%WFPS) would be function of soil organic matter (SOM) quality. SOM quality was measured by particulate organic matter (POM) and mineral-associated organic matter (MAOM) SOM proportions (next to dissolved OM as third fraction as well) for a consistent set of 10 light textured cropland soils.

The findings reveal an immediate surge in carbon mineralization post-rewetting, consistent with the Birch effect. Cumulative carbon mineralization and relative cumulative mineralization patterns exhibit an initial rapid rise followed by stabilization, indicating an equilibrium shift.Through the utilization of a parallel first- and zero-order kinetic model in conjunction with correlation analyses, we gained insight into the effects of soil moisture, the SOM fractions, and total organic carbon on mineralization rates. POM and MAOM fraction proportions correlated with the C mineralization rate constants, emphasizing the role of SOM quality. However parameters of a Gaussian function describing the Rh – WFPS relations found no relation between the its model parameters and the these organic matter fractions. Contrary to our hypothesis we did not observe mediation of the moisture dependency of SOC mineralization onto its quality.

1. INTRODCTION

1.1 Background

The Intergovernmental Panel on Climate Change (IPCC) has recently published a latest report, AR6 Synthesis Report-Climate Change 2023(Calvin et al., 2023), emphasizing that limiting global temperature increase to a specific level requires limiting cumulative net CO_2 emissions to within a finite carbon budget, along with strong reductions in other GHGs and that current mitigation and adaptation actions and policies are not sufficient.

Soil is crucial for the global carbon cycle, serving as the second-largest carbon reservoir of the fast C-cycle after the ocean and the largest store of terrestrial carbon. In the global soil carbon pool, soil organic carbon (SOC) accounts for approximately 62%, while soil inorganic carbon (SIC) accounts for 38% (Lal, 2004; Stockmann et al., 2013). Due to its associated benefits to agriculture and the substantial amount of carbon agricultural soils could sequester, increasing SOC sinks and reducing CO_2 emissions in agricultural land has been forwarded as an appealing strategy for mitigating climate change. An assessment (Bossio et al., 2020) revealed that soil carbon represents 25% of the potential of natural climate solutions (total potential, 23.8 Gt of CO_2-equivalent per year) and comprises 47% of the mitigation potential of agriculture and grasslands.

Restoration of SOC in agricultural lands will necessitate adapted management with a positive C balance: i.e. inputs of C exceed the losses by primarily decomposition. Organic matter decomposition involves biochemical processes where carbon is released as CO_2 after mineralization or transformed into recalcitrant forms by microbes, significantly impacting atmospheric carbon levels (Raza et al., 2023). Microorganisms are the primary agents of OM decomposition and are often responsible for greater than 90% of the total heterotrophic respiration (Sanderman & Amundson, 2014). To effectively enhance soil organic carbon (SOC) restoration, a comprehensive grasp of how environmental factors govern SOC mineralization would be helpful. This understanding has been partly incorporated into soil carbon models, enabling the projection of SOC dynamics in scenarios such as climate change. Notably, in the context of simulating the impact of changing climate in particular the control of temperature and soil moisture on SOC mineralization need to be properly modelled.

While extensive research has been dedicated to scrutinizing the impact of temperature on the mineralization of soil organic carbon (SOC) and its fractions, the influence of soil moisture on SOC mineralization has predominantly treated SOC as a single and unified pool

(Védère et al., 2022). In reality, it is widely recognized that soil organic matter (SOM) is characterized by significant complexity, and consists of multiple pools or fractions that are distinct based on their biochemical and physical properties, as well as their biodegradability. Further exploration of the soil moisture-heterotrophic respiration relationship on the level of such individual SOC components would be meaningful in that it could enable us to unravel the intricate mechanisms of carbon dynamics in ecosystems, predict responses to climate change, and optimize land management practices.

1.2 Objectives and approach

1.2.1 Objectives

Recent research (Bosatta & Ågren, 1999) emphasizes the importance of considering soil organic matter (SOM) quality, which refers to how readily the carbon present in the organic matter can be mineralized, to understand how management and the environment affect soil carbon storage and rate of mineralization of nutrients. In this context, SOM has often been separated into operational physical fractions, such as particulate organic matter (POM) and mineral-associated organic matter (MAOM) (Yu et al., 2022). However, whether or not and how the soil moisture-heterotrophic respiration relationship depends on SOM quality remains poorly understood.

An increase in the proportion of particulate organic matter (POM) in soil organic matter (SOM) might lead to higher heterotrophic respiration rates under similar soil moisture and temperature conditions in a laboratory setting. Also the higher the moisture content, the higher the heterotrophic respiration rate until a plateau level around 50-60% of water-filled pore space level (WFPS). These trends are well reported and are not the prime subject of this research, but instead this thesis' **main goal** was to study how SOM quality affects the soil moisture-heterotrophic respiration relationship.

Our central hypothesis was that the soil moisture – SOC mineralization relationship would be altered by SOC quality in the following manner: A higher relative POM content (at the expense of MAOM) would bring about a stronger dependency of SOC mineralization to %WFPS in the drier WFPS range (from 0-50 %WFPS) because larger sized POM resides by default in large pores in which soil moisture could limit microbial activity, while finer MAOM resides in finer pores where microbial activity is nearly never limited by available moisture, even in drier soil.

1.2.2 Approach

The above objective and connected hypothesis were investigated by quantifying SOC mineralization dependency to volumetric moisture content under controlled lab conditions in a comprehensive soil incubation experiment. For this research, a set of soils with comparable SOC content and light soil texture but variable proportions of POM and MAOM was specifically selected. This then allowed to in isolation quantify moisture dependency of SOC mineralization. This was done by fitting non-linear models to the cumulative relative SOC mineralization in function of % WFPS. Relations between derived kinetic C-mineralization model parameters and the relative proportions of MAOM and POM were then investigated to test the central hypothesis.

2. LITERATURE REVIEW

2.1 Soil organic matter

2.1.1 Nature of SOM

Soil organic matter (SOM), formerly known as humus (Paul, 2016), as defined in the "Encyclopedia of Analytical Science" (Second Edition) (Bernoux & Cerri, 2005), is the organic fraction of the soil that excludes undecayed plant and animal residues, but can also encompass the total organic material present in soils, including living microorganisms and undecayed residues in a broader definition.

The historical evolution of soil organic matter comprehension includes ancient soil categorization by color, early fractionation efforts, acknowledgment of biological and abiotic impacts, and insights into decomposition dynamics (Paul, 2016). In the contemporary perspective, SOM has similar, worldwide characteristics, but varies with abiotic controls, soil type, vegetation inputs and composition, and the soil biota, and it contains both carbohydrates, as well as proteins, lipids, phenol-aromatics, protein-derived and cyclic nitrogenous compounds, and some still unknown compounds (Paul, 2016).

Comprehending the nature of SOM entails recognizing its formation and dynamics controls, with chemical composition (recalcitrance), physical shielding, and matrix interactions (involving clay, silts, sesquioxides, and cations) frequently highlighted as central factors influencing SOM formation and dynamics (Paul, 2016).

2.1.2 Formation of SOM

Three competing models regarding the fate of organic inputs to soil were be distinguished (Lehmann & Kleber, 2015): The Humification Model, the Selective Preservation Model, and the Progressive Decomposition Model.

The Humification Model, the oldest among the three concepts, proposes that following initial decomposition of plant and soil materials, a subsequent transformation generates large, dark "humic substances," initially considered carbon and nitrogen-rich structures specific to humification, resistant to decomposition and perceived as older components of

SOM. However, its validity and the physical existence of these substances beyond specific extraction methods have been contentious and largely this model is no longer widely accepted.

The Selective Preservation (Preferential Decomposition) Model, a more recent concept influenced by studies on leaf and visible plant fragment decomposition in soils, suggests that organic inputs comprise both labile (easily decomposable) and relatively recalcitrant (more resistant) compounds, with microorganisms initially decomposing labile compounds before turning to the more resistant ones once labile sources are depleted. However, contemporary research questions the notion of rigid recalcitrance, revealing that apparently persistent materials can be broken down relatively rapidly by specialized decomposers under suitable conditions.

The Progressive Decomposition Model (also referred to as the biopolymer degradation or degradative concept) posits that SOM comprises a diverse array of organic fragments and microbial products at varying degrees of decomposition; the so-called alkali-extracted "humic substances" are now in fact considered to be a composite of identifiable compounds, including plant and microbial fragments, distributed within micro-aggregates, challenging the notion of a distinct humic fraction. This model underscores that during organic matter decomposition by microorganisms, the materials follow an energetically downward trajectory, in contrast to the hypothetical "humic substances" proposed by the humification model.

2.1.3 Stabilization mechanisms explaining persistence of SOM in soil

While it has been traditionally believed that the molecular structure of biomass and organic material dictates long-term decomposition rates in mineral soil, recent advancements in analysis and experimentation have revealed that molecular structure alone does not control SOM stability, and in fact, environmental and biological factors play a dominant role in controlling soil organic matter stability (Schmidt et al., 2011). It specifically posited asserted specifically that protection of transformed plant residues and microbial products occurs through spatial inaccessibility-resource availability, aggregation of mineral and organic constituents, and interactions with sesquioxides, cations, silts, and clays (Paul, 2016). Notably, the physicochemical adsorption of organic matter onto soil minerals, resulting in the formation of mineral-associated organic matter (MAOM), stands out as a key mechanism contributing to the stabilization of SOM (Islam et al., 2022).

2.1.4 Importance of SOM

Although constituting a minor fraction of agricultural soil mass, soil organic matter is linked to enhanced soil structure (King et al., 2020). Originally centered on soil fertility, the positive effect on crop yield, and later extended to interactions with heavy metals due to soil contamination, SOM research underwent a shift in the 1980s towards carbon sequestration in response to growing awareness of global warming (Hoffland et al., 2020). Despite this, SOM's role encompasses a broader spectrum of physical, chemical, and biological processes vital for ecosystem functions beyond carbon sequestration, providing nutrients, energy, erosion protection, biodiversity habitat, primary production, climate regulation, and compound retention as ecosystem services(Hoffland et al., 2020).

2.2 SOC Balance

Alterations of the SOC stock results from the equilibrium between the creation of new SOC and the depletion of existing SOC (Chen et al., 2022; Olson, 1963).

2.2.1 Carbon inputs

Organic matter influx into soils originates mainly from plants, involving ongoing root exudation, root tissue turnover, and deposition of aboveground plant residues, with highly variable amounts dictated by spatial, temporal, and ecosystem factors. Furthermore, plants channel organic carbon to mycorrhizal symbionts, which play a significant role in contributing organic carbon to the soil (Cotrufo & Lavallee, 2021; Godbold et al., 2006).

The type of vegetation and land use practices can alter the quantity and quality of organic matter inputs to the soil, affecting microbial communities and CO_2 emissions. An investigation centered on two chinampa ecosystems with varying natural grass covers, revealing that plant biomass influenced CO_2 fluxes seasonal variability (Ikkonen et al., 2020). Another study observed temporal changes in soil respiration (SR) spatial patterns in a Leymus chinensis dominated grassland, noting significant variation across observations, influenced by plant and microbial biomass, particularly in July(Shi et al., 2020).

The introduction of certain organic or mineral substances into the soil triggers a significant and relatively rapid change in the turnover of soil organic matter, resulting in the accelerated release or immobilization of carbon (C), nitrogen (N), and other nutrients in the soil, a phenomenon recognized as the priming effect (Kuzyakov et al., 2000). The existence of such priming effects complicates predicting the net effect of C inputs, while contributing to formation of SOC, they also stimulate decomposition of older native SOM.

2.2.2 Carbon output

Soil CO_2 flux, as the second-largest carbon flux in terrestrial ecosystems, plays a pivotal role in regulating atmospheric CO_2 concentrations and acts as a vital process bridging belowground and aboveground carbon cycling within these ecosystems (Wang et al., 2010; Wang et al., 2020). This flux results from the combined effects of biotic respiration and

abiotic geochemical CO_2 exchange, encompassing both autotrophic and heterotrophic CO_2 fluxes arising from various sources in the soil, including plant roots, soil microbes, and other soil fauna (Wang et al., 2010; Wang et al., 2020). Soil surface CO_2 flux (Rs) is overwhelmingly (almost entirely), the product of respiration by roots (autotrophic respiration, Ra) and soil organisms (heterotrophic respiration, Rh) (Bond‐Lamberty et al., 2004; Davidson & Janssens, 2006). Autotrophic respiration is associated with root carbohydrates and root exudates, which have a short residence time in the soil, whereas the heterotrophic component involves carbon compounds with longer residence times, varying from months to years for fresh litter and from years to centuries for old SOM (Epron, 2009). And each component is believed to be influenced differently by climatic conditions and site characteristics, and their responses to elevated atmospheric CO_2 or soil warming are also expected to differ (Epron, 2009). While much study has already focused on the temperature dependency of the decomposition of SOM components, much less is known how the impact of other environmental factors would differ for different SOM pools.

Soil heterotrophic respiration (Rh) represents the carbon losses from the decomposition of litter detritus and soil organic matter by microorganisms (Tang et al., 2020). Decomposition of SOC could be readily quantified on the short term by monitoring Rh. **In this MSc thesis**, likewise relative decomposability of SOC was assessed by measuring soil CO_2 efflux in the lab under controlled conditions. Heterotrophic respiration (Rh) exhibits significant variation across different time scales, from daily fluctuations to seasonal cycles, and **its principal controls are soil temperature and moisture** (Nissan et al., 2023; Tang et al., 2020). Logically, soil temperature is a critical driver of microbial activity and enzymatic reactions, influencing the rate of CO_2 production through biotic respiration. As such, seasonal and spatial variations in temperature can impact HR profoundly, with many studies demonstrating a positive correlation between soil temperature and Rh, such as (Lloyd & Taylor, 1994; Nissan et al., 2023; Ren et al., 2022). The relationship between **soil moisture** and respiration rates (Rh rates) is the prime subject of **this MSc research** and will be **discussed in further detail under 2.2.3**.

2.2.3 Soil moisture and respiration rates (Rh rates)

Moisture serves as a pivotal environmental factor driving microbial heterotrophic respiration (Rh), as its influence extends across multiple soil processes encompassing microbial activity, mineral leaching, and the movement of dissolved organic matter (Moyano et al., 2013). In

their review, Moyano et al. (2013) shed light on the multifaceted influence of moisture: reduced levels obstruct solute movement, constraining microbial nutrient availability and growth, potentially triggering dormancy. Conversely, high moisture restrains soil HR rates by suppressing oxygen supply from the atmosphere due to the diffusion rate of oxygen through water is much lower than through air.

Consequently, the general **relationship between soil moisture and respiration rates** (Rh rates) takes on a non-monotonic character, resembling a **bell-shaped curve** (Fig. 1), exhibiting troughs at both moisture extremes and reaching a zenith at a specific moisture level where an optimal balance between water and oxygen availability is achieved (Moyano et al., 2013; Nissan et al., 2023; Yan et al., 2018).

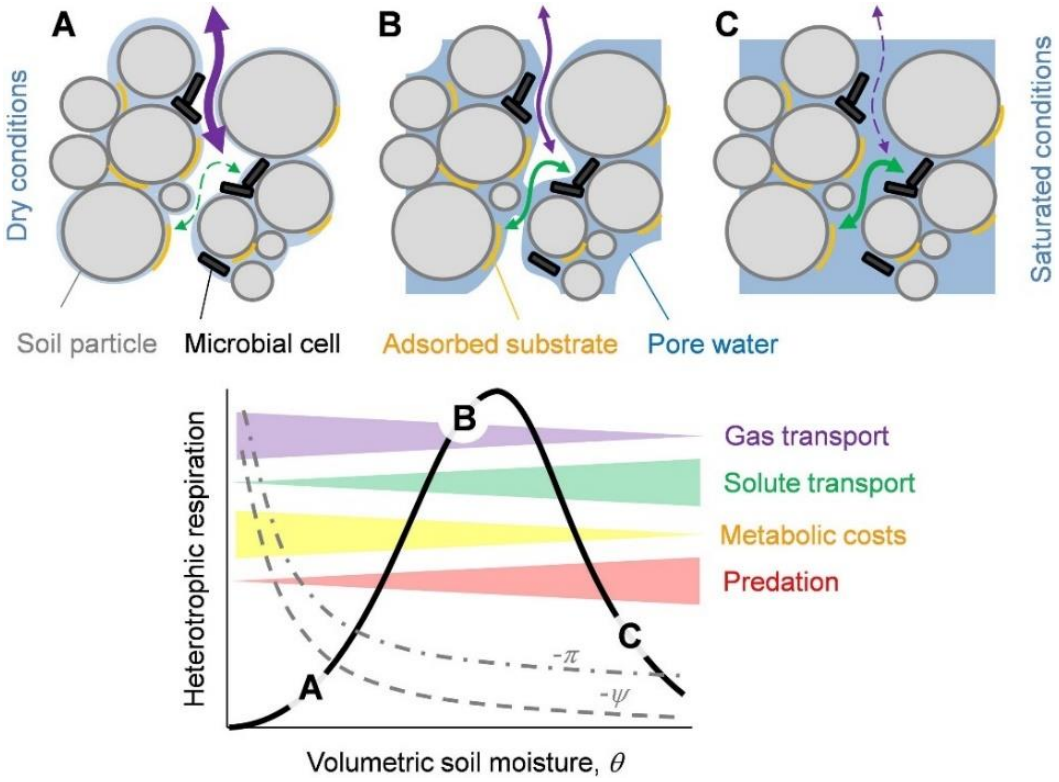

Fig. 1 *Diagrammatic representation of the impact of soil moisture on Microbial Activity (Moyano et al., 2013). The correlation between heterotrophic respiration and soil moisture levels is the cumulative outcome of various intertwined factors, spanning from limitations in diffusion to physiological, biochemical, and ecological processes. Due to the diverse and often counteracting nature of these influences (e.g., substrate transport diminishes with decreasing soil moisture, whereas oxygen transport increases), the respiration rate displays a zenith at intermediate levels of soil moisture. In the lower panel, the symbol ψ signifies the soil water potential, while π represents the cellular osmotic potential aimed at upholding stable turgor pressure amidst declining ψ.*

2.2.4 Abiotic factors affecting heterotrophic respiration rates (Rh rates)

Diverse physical and chemical soil attributes, encompassing factors like soil particle size, pore space arrangement, and organic matter content, could contribute to the variability in microbial respiration response to moisture through influencing factors such as water thresholds and the diffusion of gases and solutes (Moyano et al., 2013). Notably, particle size significantly shapes soil water retention, with higher clay content enhancing water-holding capacity but possibly limiting free water availability for substrate diffusion and respiration. Soil pore space, inversely linked to bulk density, crucially affects gas diffusion, and higher porosity reduces oxygen constraints. Additionally, soil organic matter content modifies the relationship between soil respiration and moisture by altering water retention, pore space, and microbial activity rates (Moyano et al., 2013).

While some knowledge thus exists on how SOM content, porosity and soil texture mediate the soil moisture soil heterotrophic relationship, the influence of **SOM quality** remains a blank spot and will be further considered **in this thesis**. **For such research it will also be important to keep the factors SOM content, texture and bulk density as far as possible constant.**

2.3 SOM Fraction and pools

The study of soil organic matter (SOM) components dates back to the early 1800s until the 1980s, focusing on chemistry and separating soluble OM compounds into humic and fulvic acids (Kögel-Knabner & Rumpel, 2018). In the 1990s, research shifted towards understanding the biological processes influencing SOM formation and dynamics, introducing techniques like physical fractionation and molecular analysis, which now enable detailed assessments of SOM composition, origin, and turnover in specific soil locations (Kögel-Knabner & Rumpel, 2018; Poeplau et al., 2018). An exploration of 20 soil organic carbon (SOC) fractionation methodologies conducted on agricultural soils experiencing vegetation changes demonstrated that a combined physical and chemical approach effectively separates SOC fractions with varying turnover rates(Poeplau et al., 2018). However, in particular current SOM fractionation methods face challenges in achieving homogeneous or functional OM pools due to an unclear linkage of these fractions to stabilization mechanisms (Lützow et al., 2007). In addition, an discussion highlighted that the numerous fractionation methods used in soil studies make it challenging to quantitatively compare results and establish standardized protocols due to the wide variation in soil properties and SOC stabilization mechanisms, making it unlikely that a single optimized method will suit all soils; hence, it remains challenging to determine the most efficient method for separating fractions with distinct properties (Poeplau et al., 2018).

But within comparable land-use and soil type, fractionation methods could reveal meaningful information on SOM quality. A framework was proposed that dividing SOM into particulate (POM) and mineral-associated (MAOM) forms, because these two SOM components differ fundamentally in their formation, persistence and function (Lavallee et al., 2020). Such a rather simple approach could already start to help to address challenges posed by diverse SOM separation schemes that hinder cross-study comparisons and broad-scale generalizations, offering benefits such as clearer communication, consistent separation, cost-effectiveness, and improved predictions of SOM dynamics, guiding land managers and policymakers in managing SOM amidst global change challenges.

In this MSc thesis research, we adopt the simple conceptualization of SOM being primarily in the forms of particulate (POM), mineral-associated (MAOM), and — as a much smaller proportion, i.e., 1–2% — dissolved organic matter (DOM).

POM is a fraction of SOM primarily composed of structural materials from plants and microbes that have undergone fragmentation and leaching losses but limited depolymerization, characterized by its relatively light and coarse nature with densities <1.6–1.85 g cm^{-3} or sizes >53 µm (Leuthold et al., 2023). And POM in the soil matrix is

predominantly unbound and protected from decomposition by its chemically recalcitrant components and occlusion within aggregates, leading to a relatively short average residence time in agricultural soils, ranging from years to decades (Just et al., 2023a),.

Mineral-Associated Organic Matter (MAOM) is formed through chemical interactions between SOM and mineral surfaces, along with its confinement within micropores or small aggregates < 53 µm, effectively rendering the SOM inaccessible to decomposers, thus contributing to its long-term stability in the soil environment (Mirabito & Chambers, 2023a). MAOM stands as a more durable and resilient form of SOM, demonstrating persistence over extended periods, ranging from centuries to millennia, while displaying resistance to alterations in environmental conditions (Lützow et al., 2007; Rocci et al., 2021). Its inherent stability plays a crucial role in preserving SOC stocks and contributing to the overall carbon cycling dynamics in the face of changing global conditions.

Dissolved Organic Matter (DOM) is defined as the fraction of organic matter in solution that passes through a 0.45 µm filter, despite being a small fraction of total organic matter in soil, significantly influences biogeochemical processes in both terrestrial and aquatic environments, with its production, transport, and interactions serving as sensitive indicators of ecological shifts (Bolan et al., 2011).

3. MATERIALS AND METHODS

In this section, we outline the experimental setup and methodology employed to investigate the effect of soil organic matter (SOM) quality on the relationship between soil moisture and carbon mineralization.

This section begins by introducing a dataset concerning the quality of SOM, obtained from soil samples collected within a previous study on the Flemish Luikbeek stream basin (section 3.1). Next, a meticulous selection of 10 soils exhibiting consistent texture and SOC content, while displaying variations in the relative proportions of POM and MAOM, is described (section 3.2). Section 3.3 outlines the implementation of a controlled laboratory incubation experiment to evaluate carbon mineralization rates, detailing the experimental setup and moisture regulation. Section 3.4 elaborates on the analysis of CO_2 concentrations in soil gas samples using gas chromatography and subsequent unit conversion, serving as a foundation for calculating relative cumulative C-mineralization rates. Finally, in Section 3.5, a kinetic C-mineralization model is introduced to fit cumulative relative C-mineralization data while incorporating soil moisture dynamics through the utilization of a Gaussian function

3.1 Dataset on SOM quality

In 2013, a study led by the Soil Fertility and Nutrient Management Research Group at the Faculty of Bio-Engineering Sciences, Ghent University, aimed to investigate whether quantitative information on SOM composition could enhance the prediction of N mineralization in a series of arable soils within the Luikbeek stream basin (Province of East Flanders). In this study carried out for INAGRO soil samples collected from 39 fields cultivated with field vegetables in the spring of 2013 were investigated for their mineral N supply (Fig. 2).

During that study, a soil fractionation scheme was employed to subdivide soil C and N and in doing so assess variation in the SOM quality (Fig. 3). Air-dried soil samples were subjected to physical and chemical fractionation, which resulted in the separation of several meaningful soil fractions. Initially, the complete soil sample (30g) underwent mild ultrasonic dispersion at 60 J ml^{-1} and was then separated through wet sieving into a sand fraction (>50µm), a silt+clay fraction (<50µm), and a water-soluble fraction.

The <50µm fraction was moreover further split into oxidizable and oxidation resistant parts and a part that could be extracted with hot water. This further subdivision of the silt and clay sized fraction, as well as the two separated DOC fractions will not be considered for **the present MSc thesis research**. The relative proportion of the sand C fraction is taken to equal POM C and that of the silt and clay fraction is taken equal to MAOM C.

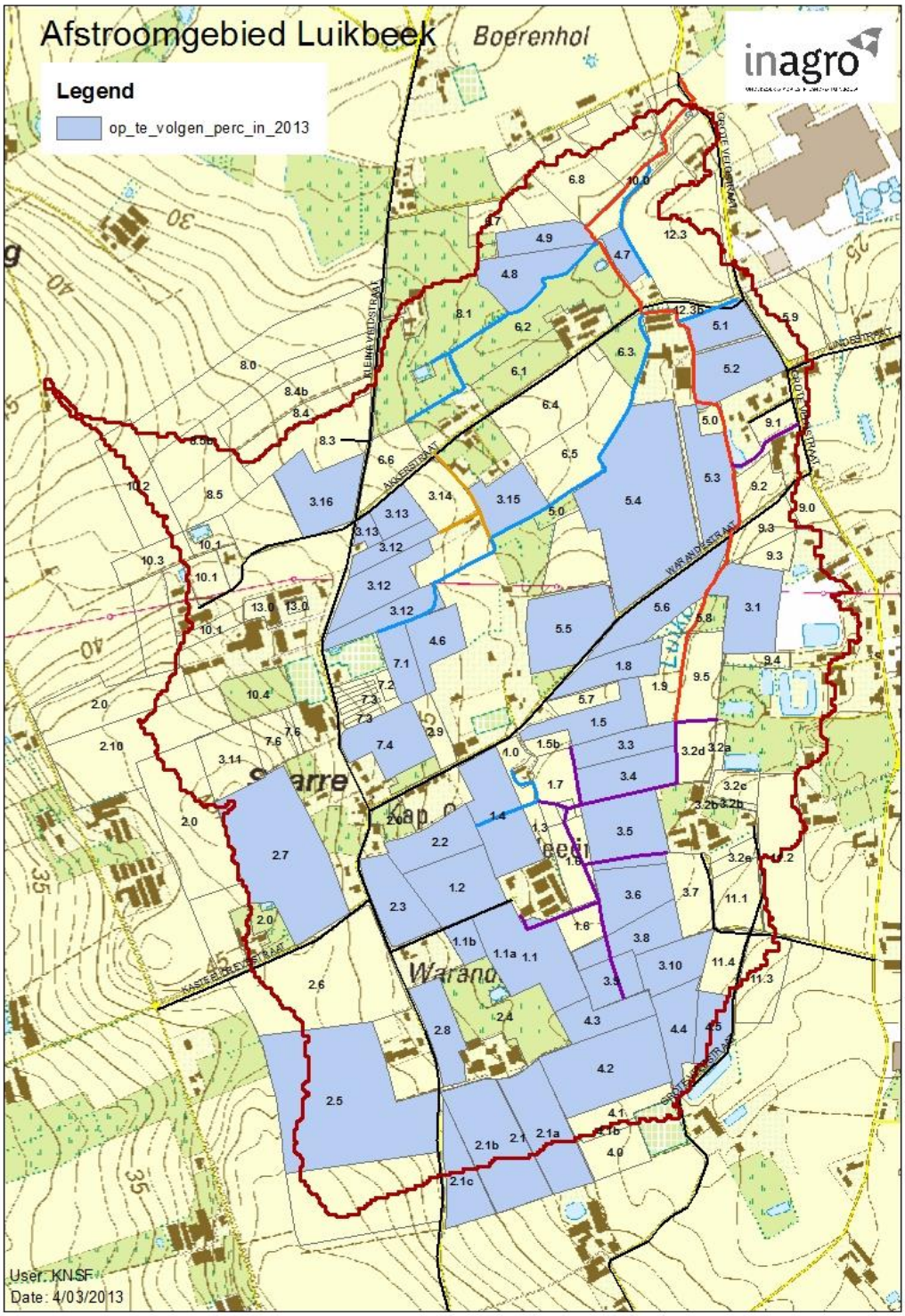

Fig. 2 *Location of the 39 sampled agricultural plots in the Luikbeek stream basin during a previous study conducted by the Soil Fertility and Nutrient management research group (UGhent) for INAGRO*

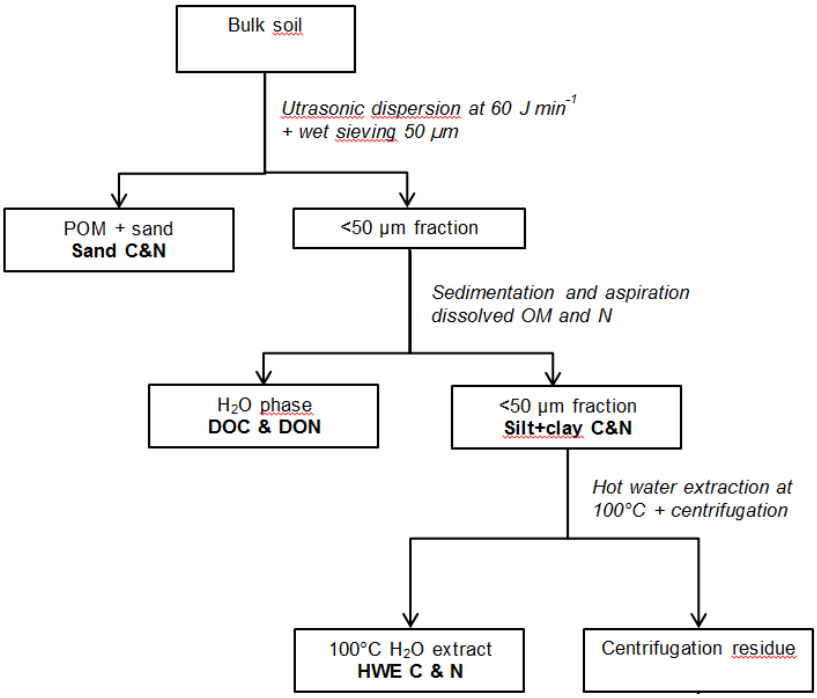

Fig. 3 *Fractionation scheme for the sequential separation of C and N into free particulate OM (sand C & N); water soluble OM (DOC & DON); hot-water extractable OM (HWE C & N); NaOCl oxidizable – and resistant OM (6% NaOCl-ox C&N; 6% NaOCl-res C&N) during a previous study conducted for INAGRO to assess variation in SOM quality in the Luikbeek catchment.*

3.2 Selection of soils

The soils used in this study consisted of air-dried soil samples inherited from the above described Luikbeek study. Our central goal was to investigate the dependency of the soil moisture - Rh relationship on SOM quality in agricultural soils. To in isolation assess the effect of SOM quality we accordingly selected a consistent set of soils with well comparable management history and soil texture and limited variation in SOC content. For this a specific selection was made out of the 39 previously analysed Luikbeek cropland fields.

Since soil texture had not been determined, the digital Belgian soil map was firstly used to assign soil textural classes to each of the 39 fields. For this the 'Bodemverkenner' website (Fig. 4), accessible at https://www.dov.vlaanderen.be/portaal/?module=public-bodemverkenner, was utilized. Only soils with texture varying between loamy sand (symbol S in the Belgian soil classification) and light sandy loam (P) were further considered for this thesis research.

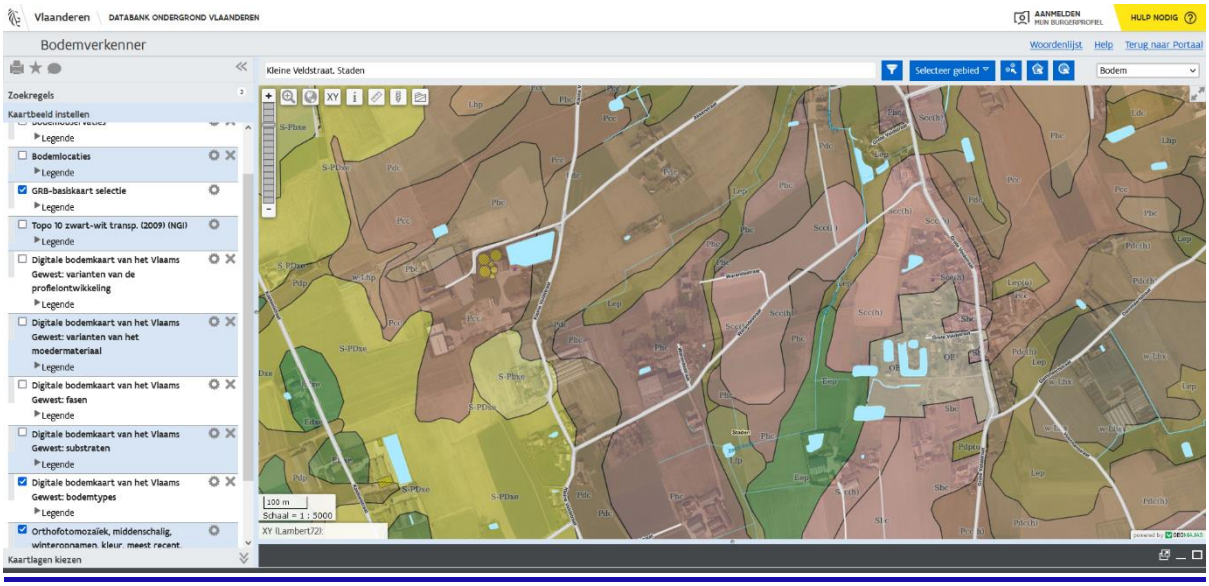

Fig. 4 *The digital Belgian Soil map (on the Bodemverkenner website) overlain on aerial photo of part of the 'Luikbeek' catchment.*

Data on SOC content was extracted from the aforementioned previous Luikbeek study, including total soil organic carbon (TOC) and the relative share of isolated soil C fractions, such as the relative share of POM and MAOM C. In accordance with the objectives of experiment and the availability of soil materials, we then carefully chose 10 soils with as far

as possible similar soil texture and SOC content but varying relative SOM proportions of MAOM and POM. The properties of the final selected soil materials are presented in Table 1.

***Table 1**: Soil texture, SOC total content (TOC) and contents of DOC, MAOM and POM of the 10 cropland topsoil materials selected for this MSc thesis. The relative proportion of POM is also given as % of SOC in the last column (Belgian classification of soil texture: S = loamy sand, P = light sandy loam)*

Soil Sample Number	Soil Texture	TOC (g /kg)	DOC (g /kg)	MAOM (g /kg)	POM (g /kg)	POM fraction
1-4	P	14.95	0.15	11.61	3.19	21.3%
2-3	P	13.25	0.13	9.55	3.57	26.9%
2-5	P+S	9.15	0.10	6.49	2.56	28.0%
2-8	P	10.55	0.07	7.81	2.68	25.4%
3-1	S	9.57	0.18	5.54	3.85	40.3%
3-13	P	10.16	0.08	6.79	3.30	32.4%
3-15	P	15.00	0.12	11.08	3.81	25.4%
4-2	P+S	13.57	0.17	11.45	1.95	14.4%
4-5	S	14.44	0.08	6.68	7.68	53.2%
4-8	P	10.15	0.15	7.71	2.29	22.6%

3.3 Soil incubation experiment

3.3.1 General description

Laboratory incubation with measurement of CO_2 efflux is the prevalent method for measuring soil organic carbon (SOC) mineralization and studying the impact of environmental factors on different carbon pools, with experiment durations ranging from hours to years (Guan et al., 2022).

In this study, our primary objective is to explore the intricate relationship between soil organic matter quality and the influence of soil moisture on SOC mineralization. To do so SOC mineralization was assessed by measuring soil heterotrophic respiration on the set of 10 cropland soil with variable MAOM and POM proportions in function of soil moisture content. Heterotrophic respiration was assessed from the evolution of soil CO_2 efflux under controlled conditions during 60 days in the laboratory. A constant temperature of 15°C was maintained throughout by incubating the soils inside two incubation cupboards. Additionally, we standardized the physical disturbance and bulk density, ensuring that each sample possessed similar soil porosity.

To ensure comparable soil structure between the 10 used soils they were treated with first a likewise disturbance of the soil structure by sieving at 2mm and then repacking soil inside PVC tubes at a fixed soil bulk density with a closed bottom. The density was set at 1.35 g/cm^3, which approximates a typical density of cropland topsoil in the field for sandy loam soils. Soil Porosity = (1 - (Bulk Density ÷ Particle Density)) x 100 and was thus 49%. Details on the resulting soil columns used in the incubation experiment are summarized in Table 2.

***Table 2**: Specifics of the soil mesocosms*

Soil bulk density (g/cm^3)	1.35
Diameter of PVC tubes (cm)	6.8
Height of filled soil in tube (cm)	5.0
Soil volume in tube (cm^3)	181.58
Soil porosity	49%
Soil Weight in tube (g)	245.14

More specifically preparation of the soil mesocosms inside PVC tubes went according to the following specific experimental steps:

I. We measured 245.14g of soil and added a calculated amount of water to achieve the desired moisture level (see 3.3.2 and Tabel 3) in a bowl.
II. The soil and water were mixed thoroughly with a spoon to ensure homogeneous moisture distribution.
III. The moist soil was put into the PVC tube (with a bottom cap) and then compacted to a height of 5 cm to obtain the desired bulk density.
IV. The tubes were sealed with Parafilm foil wherein small holes were punctured using a needle to allow sufficient gaseous exchange, whilst limiting evaporative loss of soil moisture.
V. Finally, the tubes were placed in the incubation cupboard with fixed temperature and moisture conditions. At onset and further on during the incubation experiment the air in the incubation cupboard was humidified by letting an air humidifier run for 15 minutes, as depicted in Fig. 5. This was done to further limit evaporation from the soil cores.

Fig. 5 *Incubation Cupboard Setup with Soil Cores and Air Humidifier*

3.3.2 Setting a target range for soil moisture levels

We varied soil moisture content during the incubations by repeating the same incubation experiment on all 10 soils for a range in soil moisture levels. This then allowed to investigate how different SOM qualities interacted with the effect of moisture on SOM mineralization. To express the soil moisture, two key metrics were employed: the Water-filled pore space percentage (WFPS %) and the volumetric soil water content (SWC). Volumetric Soil water content (SWC) is the volume of water per unit volume of soil:

SWC (%) = [volume of water /volume of soil] × 100

Water-filled pore space (WFPS) is defined as the ratio of volumetric soil water content to the total soil porosity, representing the proportion of water volume in the soil pores relative to the entire pore space (including both water-filled and air-filled pores):

WFPS % = (volume of water / Total volume of pore space) x 100

For example, when considering a specific scenario with the following soil characteristics: the soil volume in the tube measures 181.58 cm^3, and the soil porosity is 49%, resulting in a total volume of all soil pores of 88.97 cm^3. At 10% WFPS, the volume of water in the soil pores was approximately 8.9 cm^3, corresponding to a mass of 8.9 g. The SWC, calculated as the percentage of water volume to total soil volume, is then 4.9%.

In this MSc research we focused on the 'dry' end of the bell-shaped Rh-moisture relationship: i.e. from 0 to 60 %WFPS, which is often the optimum %WFPS for SOC mineralization in light-textured soils. Six different moisture steps (next to dry soil) were considered, viz. 10, 20, 30, 40, 50 and 60% WFPS. Appropriate amounts of deionized water were added to the soils achieve these desired soil moisture levels, as detailed in Table 3.

***Table 3**: Amount of water added to the soil cores to obtain a range in Soil Moisture for the soil incubation experiments*

Water-filled pore space (WFPS) %	0	10	20	30	40	50	60
Soil water content (SWC) %	0.0	4.9	9.8	14.7	19.6	24.5	29.4
Added water (ml)	0.0	8.9	17.8	26.7	35.6	44.5	53.4

This experiment was duplicated, resulting in a total of 120 soil cores through the combination of 10 soil types, 2 laboratory replicates, and 6 distinct soil moisture levels.

During the experiment, soil cores were regularly weighted and upon significant weight loss, they were brought back to their initial staring weight by adding deionized water.

3.3.3 Heterotrophic respiration measurements

After preparation of the soil mesocosms in the PVC tubes and their placement in the controlled incubation cupboard environment, the incubation phase initiated. The heterotrophic respiration rate of all soil samples was measured periodically throughout the incubation period, as shown in Table 4. For practical reasons the experiment was completed in two separate batches.

***Table 4**: Temporal sampling schedule for diverse WFPS levels in two separate batches during incubation*

Days Since Experiment Start	Time Interval with Last Experiment Day	Testing Date - Moisture Level WFPS 20%, 40%, 60%	Testing Date - Moisture Level WFPS 10%, 30%, 50%
0			
2	2	04/26/2023	05/11/2023
5	3	04/29/2023	05/14/2023
9	4	05/03/2023	05/18/2023
14	5	05/08/2023	05/23/2023
21	7	05/15/2023	05/30/2023
28	7	05/22/2023	06/06/2023
38	10	06/01/2023	06/16/2023
50	12	06/13/2023	06/28/2023
64	14	06/27/2023	07/12/2023

The procedure for measuring the soil heterotrophic respiration rates was as follows:

I. The soil mesocosm (Parafilm covered soil core in a PVC tube) was taken from the incubation cupboard and transferred into a sealable canister (1L PE plastic wide mouth screw cap pots).
II. The Parafilm was removed to allow free CO_2 efflux and soils were kept in open pots for about 15min to evacuate excess CO_2 that had accumulated inside the incubation cupboards.

III. A first small air sample (20ml) was collected with a 25ml plastic syringe with a needle attaced to measure the initial concentration of carbon dioxide (CO_2) inside the pot. This 20ml gas sample was injected into a pre-evacuated 12ml Exetainer vial for storage until analysis of the CO_2 concentration with the GC. The overpressure applied during injection ensures limited further leakage of air into the Exetainer further on.

IV. The PE pot was closed with a lid outfitted with a rubber septum (in a glass tube attached to the lid of the PE pot through a pierced stopper) to initiate accumulation of emitted CO_2 in the inner 1L headspace.

V. By piercing the septum with the syringe needle a second headspace air sample was collected from the pots after a first 20-minute sealing period. This gas sample was represent the accumulated CO_2 after 20min and was likewise transferred minutes into an exetainer vial.

VI. After a second 20-minute period (with the pots still sealed), another air sample was taken to record the CO_2 buildup in the headspace air after 40min.

VII. Once the gas extraction process was complete, the tubes were taken from the pots, covered again with pierced Parafilm and replaced into the controlled environment inside the incubation cupboards.

Fig. 6 *Configuration for headspace CO_2 measurement – grey tube (Left) containing soil sample, larger white PE pots outfitted with a septum (left) in which the soil cores were periodically placed for measuring headspace CO_2 buildup and gas sampling with the a syringe (right)*

3.4 CO_2 concentration analysis and soil respiration rate calculation

3.4.1 Accurate quantification of CO_2 concentrations through Gas Chromatography

The CO_2 concentrations in the gas samples were analyzed using gas chromatography (GC), an Agilent 7890 GC equipped with an Electron Capture Detector (ECD), Flame Ionization Detector (FID), methanizer, and three valves. In this approach, 1ml gas samples are consecutively introduced into the GC system by an autosampler. By establishing the peak retention time and area of the precise concentration of CO_2 in the test sample can be accurately determined with a calibration curve.

The GC CO_2 data is reported in terms of relative peak areas on the GC chromatogram. By measuring three certified CO_2 gas standards (750, 1500 and 2500 ppmv) alongside with the GC analyses a linear relation between peak area and CO_2 concentration (in ppmv) was obtained, as exemplified in Fig. 7. A fresh calibration curve is created after every 100 samples, and these calibration curves were used to convert these peak areas into CO_2 concentrations expressed in parts per million by volume (ppmv, i.e. µL CO_2 L^{-1}). Utilizing this regression curve, the CO_2 concentrations of soil gas samples collected at time points t = 0, 20, and 40 minutes during each measurement day are computed.

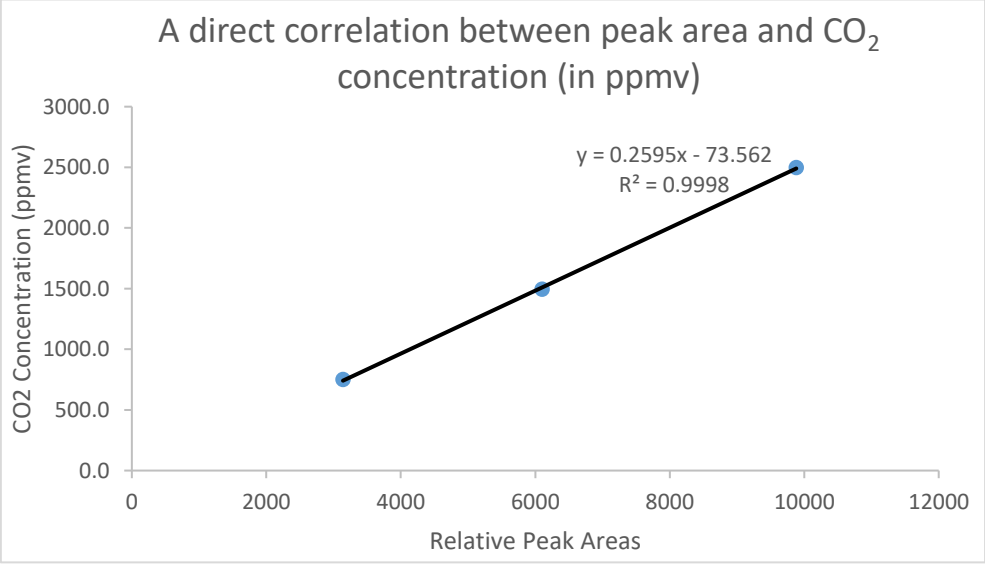

Fig. 7 *A demonstration of the calibration curve linking GC Chromatogram peak areas to CO_2 concentrations*

3.4.2 Converting the ppmv to milligrams per cubic meter (mg/m³) for CO2 using the ideal gas law

The computed CO_2 concentrations of the collected soil gas samples were initially expressed in parts per million (ppmv). To provide a clearer representation of the generated mass of CO_2, we opted to conduct a unit conversion. For this purpose, the following formula was employed:

$mg/m^3 = (44.01 / 22.41) * (273.15 / (273.15 + 15)) * (101325 / 101325) * ppm$

This conversion process utilizes the fundamentals of the ideal gas law, and the step-by-step derivation formula is as follows:

a) Initiate with the fundamental equation of the ideal gas law: PV = nRT
b) In this equation: P signifies Pressure (in Pascals, Pa); V signifies Volume (in cubic meters, m^3); n signifies the Number of moles of the gas; R signifies the Ideal gas constant (8.314 J/(mol K)); T signifies Temperature (in Kelvin, K)
c) Rearrange the equation to solve for the number of moles (n): n = PV/RT
d) Take into account the mass (m) of gas that relates to the number of moles (n) and the molar mass (M) through the equation: m = n * M
e) Substitute the expression for n from step 2 into the equation for m: m = (PV / RT) * M
f) Divide both sides by the volume (V) to derive mass per unit volume (mg/m^3): mg/m^3 = (m / V) = (P / RT) * (M / V)
g) Under Standard Temperature and Pressure (STP) conditions — where P = 1 atm, V = 22.41 L/mol, n = 1 mol, and T = 273.15 K — we can establish that R = PV/nT = 101325 * 22.41 / (1 * 273.15)
h) Given the molar mass of CO_2 44.01 g/mol, and with equipment operating at a temperature of 15°C, and room pressure set at the standard atmospheric pressure of 101325 Pa the formula becomes mg/m^3 = (44.01 / 22.41) * (273.15 / (273.15 + 15)) * (101325/ 101325) * ppm

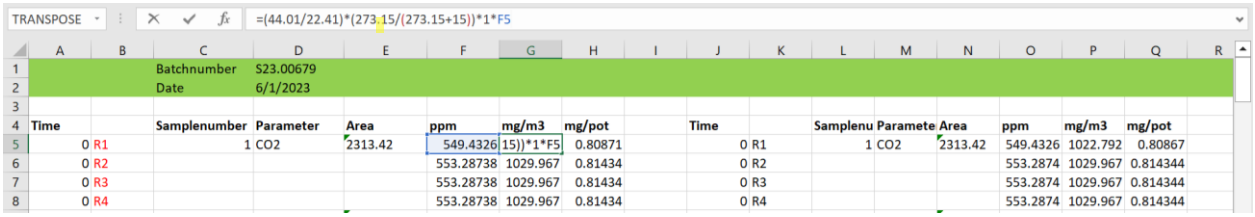

Fig. 8 *Illustrating the conversion from parts per million (ppm) CO_2 to milligrams per cubic meter (mg/m using excel formulas*

3.4.3 Converting the unit milligrams per cubic meter (mg/m^3) to milligrams per pot (mg/pot) for CO_2

After obtaining the CO_2 concentration at a particular time point, the amount or mass of CO_2 present in the headspace of each individual bottle at that specific moment can be calculated. This calculation entails multiplying the concentration by the volume of space that contains CO_2.

Using the drainage method, the volume of grey tube (shown on the left in Figure 6, is measured to be 85.85 ml and the volume of the larger white cannister (displayed on the right in Figure 6) utilized for CO_2 measurement is determined to be 1058.08 ml. During the experiment, the soil sample occupies a volume of 181.58 ml. Consequently, the specific headspace in which the CO_2 concentration was measured can be calculated as 1058.08 - 85.85 - 181.58 = 790.65 ml.

Hence, the calculation for mg/pot becomes: 0.00079065 * mg/m^3.

3.4.4 Assessing C-mineralization rates: regression analysis and conversion formula for soil CO_2 production

After obtaining the CO_2 concentrations at t = 0, 20, and 40 minutes, regression lines were fitted to describe the buildup of CO_2 over time. The slope of this regression line provides the rate of CO_2 accumulation in the pot headspace, expressed in the unit of mg CO_2/min/pot, representing CO_2 production in milligrams per minute per pot.

To establish a connection between the CO_2 production potential and the quantity of soil mass, a conversion from mg CO_2/min/pot to mg C/h/kg DS, that is C-mineralization rates in milligrams per hour on a per kg dry soil base, was implemented. And the formula is: mg C/h/kg DS = (mg CO_2/min/pot) / 3.666 * 60 / 0.24514. In this formula, The division by 3.666 in the formula is due to the fact that 3.666 mg of CO_2 contains 1 mg of C. Multiplying by 60 accounts for the conversion from minutes to hours, and the final result is divided by the weight of the soil sample, which is 0.245 kg, to present results per kilogram of soil.

To assess the reliability of the regression, we calculated the coefficient of determination (R2) for each gas measurement. Any measured CO_2 buildup trends with an R2 below 0.6 were excluded and further considered as missing data (NA). Any further calculations employed average C-mineralization rates based on both lab replicates, or upon exclusion of

measurements based on the poor R^2 criterion on just one of both replicates. Whenever negative slopes were obtained, all negative C-mineralization rates numbers were also excluded. C-mineralization rates that cannot be calculated because there was no data for either one of both replicates were also considered missing data (NA). For example, in Table 5 it is shown that several data points with poor linear buildup of headspace CO_2 were excluded from the analysis.

***Table 5** : Examples of measured R^2 and slope of linear regression lines fitted to the measured CO_2 buildup in the PE pots (data converted into mg C / h / kg). CO_2 efflux measurements with an R_2 value below 0.6 and negative values were further excluded*

	2013/5/18		2023/5/23		2023/5/30	
Gas Sample Label	R^2 (RSQ)	mg C/h/kg DS	R^2 (RSQ)	mg C/h/kg DS	R^2 (RSQ)	mg C/h/kg DS
R1	0.9699	0.2183	0.0122	NA	0.1194	NA
R2	0.7065	0.2520	0.7885	-0.1955	0.6546	0.3633
R3	0.9882	0.2454	0.4571	NA	0.9668	0.4212
R4	0.9788	0.2115	0.6531	-0.0464	0.8303	0.2887
R5	0.9981	0.3773	0.9891	0.0867	0.5517	NA
R6	0.8115	0.2817	0.2539	NA	0.7703	0.1599
R7	0.9984	0.2338	0.0069	NA	0.8974	0.1441
R8	0.9981	0.1717	0.8951	0.1088	0.9251	0.7715
R9	0.9184	0.2151	0.1834	NA	0.9689	0.3643
R10	0.9753	0.2143	0.9995	0.1223	0.8211	0.1558

3.4.5 Calculation of cumulative C mineralization and relative C mineralization rate

Following the previous treatment, C-mineralization rates were computed in milligrams per hour per kilogram of dry soil. The preceding data processing steps (exclusion of poor CO_2 trends, treating negative slopes as 0 emissions, and treating unavailable data as missing data) led to the emergence of some missing data. However, the occurrences of such missing data were limited. To enhance the accuracy of the model and address these data gaps, linear interpolation was implemented to estimate and impute missing values where deemed suitable.

To determine the cumulative C-mineralization, it is essential to account for changing rates of C mineralization over time. These rates need to be aggregated to find the total cumulative C mineralization from the start of the experiment up to each measurement day. The following

approach is applied to addresses this requirement and ensure the overall C mineralization process throughout the experiment:

I. Cumulative C mineralization (on the first measurement day):
Calculate the rate of C mineralization on the first measurement day (generally the second day of the experiment). Multiply this C mineralization rate by the time intervals between the start of the experiment and the first measurement to obtain cumulative C mineralization over the initial 2 days.

II. Calculation for subsequent measurements:
The C mineralization rate on specific days after the start of the experiment are calculated, with distinct time intervals separating these measurements.
Calculate the average C mineralization rate between the current measurement day and the previous measurement day. Multiply that average rate obtained above by the time interval between the current measurement day and the previous measurement day to gain the cumulative C mineralization rate within this time interval.

III. Adding cumulative mineralization:
For each measurement interval, calculate the cumulative C mineralization rate as described in step 2.Gradually add these cumulative rates to the previous cumulative mineralization to get the total cumulative C mineralization up to the current measurement day.

IV. Repeat for each measurement:
Repeat steps 2 and 3 for each subsequent measurement point.
Calculate the cumulative C mineralization rate for each interval and add it to the running total of cumulative mineralization.

After calculating the cumulative C mineralization, divide it by the total soil carbon content (C content) of each sample, measured in grams per kilogram (g/kg), to obtain the **relative cumulative C-mineralization, expressed as mg C/g SOC**, indicating the amount of carbon mineralized (in mg) per gram of SOC.

3.5 C-mineralization model

3.5.1 Fitting non-linear model to cumulative relative C-mineralization data

Overall, fitting a kinetic model to cumulative relative C-mineralization data allows researchers to describe and quantify the complex interplay between carbon substrates, microbial activity, and time in the context of soil carbon cycling and offer deeper understanding of the underlying mechanisms driving carbon mineralization.

We chose to use a parallel first- and zero-order kinetic model as it assumes that the SOM consists of an easily mineralizable pool of C that is mineralized following an exponential course, according to first-order kinetics, and a more resistant fraction that is mineralized according to zero-order kinetics and it is assumed that the resistant fraction is not depleted significantly during the incubation period considered (Sleutel et al., 2005). The following kinetic model (Sleutel et al., 2005) was fitted:

C_rel = ks*time + Ca*(1-exp(−kf*time))

Where:
C_rel: This parameter (mg C/g SOC) represents the cumulative relative C-mineralization over time, serving as the target value for modeling and predictive purposes.
ks: This parameter (mg C/g SOC/days) represents the mineralization rate constant of the resistant pool.
time: This is the independent variable (days) representing time, that is the input to the model and indicates the time points for collected data.
Ca: This parameter (g SOC / g SOC) show the easily degradable carbon pool.
kf: This parameter (1/days) represents the mineralization rate constant of the easily degradable carbon pool Ca.

Fitting this model to cumulative relative C-mineralization data involves finding the optimal values for the parameters ks, Ca, and kf that best match the observed data points, which is typically achieved using statistical techniques like nonlinear regression such as using the nlsLM() function in the R programming language used in this thesis. The goodness of fit was assessed by comparing the model predictions to the observed data graphically and using statistical measures like the R^2 or the root mean squared error (RMSE).

Interpreting the fitted parameters can provide valuable insights into the soil carbon dynamics. For instance, the ks parameter gives insight into the degradability of the resistant

pool, while the Ca and kf parameters reflect the decay behavior of easily degradable carbon pool over time.

3.5.2 Connecting relative C-Mineralization to soil moisture (WFPS) using Gaussian functions

Utilizing the aforementioned fitted non-linear model for Cumulative relative C-mineralization data, the cumulative relative carbon mineralization for each model at day 60 (DAY=60) was predicted.

We then investigated the relation between this relative C-mineralization data and the soil moisture content, expressed as % of Water-Filled Pore Space (WFPS). This connection can be well portrayed through a Gaussian function as also shown in previous studies at the soil fertility and nutrient management lab (De Neve & Hofman, 2002; Sleutel et al., 2008). The Gaussian function is described by the following formula:

$$rel\ C_{min-60d}(\%WFPS) = rel\ C_{min-60d;opt}\, e^{-\xi\left(1-\frac{\%WFPS}{\%WFPS_{opt}}\right)^2}$$

Where:
$rel\ C_{min-60d}(\%WFPS)$ stands for the predicted relative carbon mineralization at day 60 for a specific %WFPS value.
$rel\ C_{min-60d;opt}$: the C mineralization rate at the optimal %WFPS, which is the ideal or most conducive moisture level for carbon mineralization to occur.
e: the mathematical constant approximately equal to 2.71828
ξ: This parameter represents a coefficient that governs the shape and steepness of the decay curve, indicating how sensitive the mineralization process is to changes in moisture content.
%WFPS: the percentage of Water-Filled Pore Space
$\%WFPS_{opt}$ the optimal %WFPS, which indicates the moisture level at which the carbon mineralization process is most effective.

The formula helps illustrate how changes in soil moisture (represented by %WFPS) relative to the optimal moisture level (%WFPS_opt) impact the rate of relative carbon mineralization, by establishing an exponential decay relationship between relative carbon mineralization and %WFPS.

4. RESULTS

A thoughtfully conducted selection process was undertaken to acquire a diverse array of soil samples varying in organic matter quality but not SOC content and texture. And these soil specimens were subjected to six distinct soil moisture levels: 10%, 20%, 30%, 40%, 50%, and 60% WFPS. The resulting dataset comprised over 2000 data points, which were subsequently employed to explore the impact of SOM quality on the intricate relationship between soil moisture and heterotrophic respiration.

Below, each time two out of the 10 particular soil samples were picked to portray how the carbon mineralization rates varied across the set soil moisture range. These samples were chosen for their contrasting SOM qualities.

We begin by presenting the cumulative C-mineralization data in sections 4.1 and 4.2, followed by the fitting of kinetic C-mineralization models in section 4.3. Then, in section 4.4, we present an investigation of the connection between relative C-mineralization and soil moisture using the aforementioned Gaussian Functions.

4.1 Dynamics of C-mineralization on measurement day and evolution of cumulative C-mineralization

4.1.1 C-mineralization rates

The chosen soil samples are 1-4 and 4-5. Soil sample 1-4 contains 14.92 g/kg OC, 3.19 g/kg C as Particulate Organic Matter (POM), comprising 21.34% of SOC. Sample 4-5 contains 14.44 g/kg OC, with 7.68 g/kg POM-C, contributing 53.17% of TOC.

Fig. 9 plots the progression of the carbon mineralization rates (mg/h/kg) in soil samples 1-4 and 4-5, spanning six distinct soil moisture levels, observed at fixed time intervals after the start of the experiment. The figure illustrates that after the introduction of water at onset, C-mineralization rates undergo an initial rapid rise and reach a peak after a few days. However, over time these rates gradually decrease and eventually stabilize at lower values.

In spite of similar SOC level C-mineralization rates were generally lower in the 4-5 soil with higher POM-C content, actually against expectation.

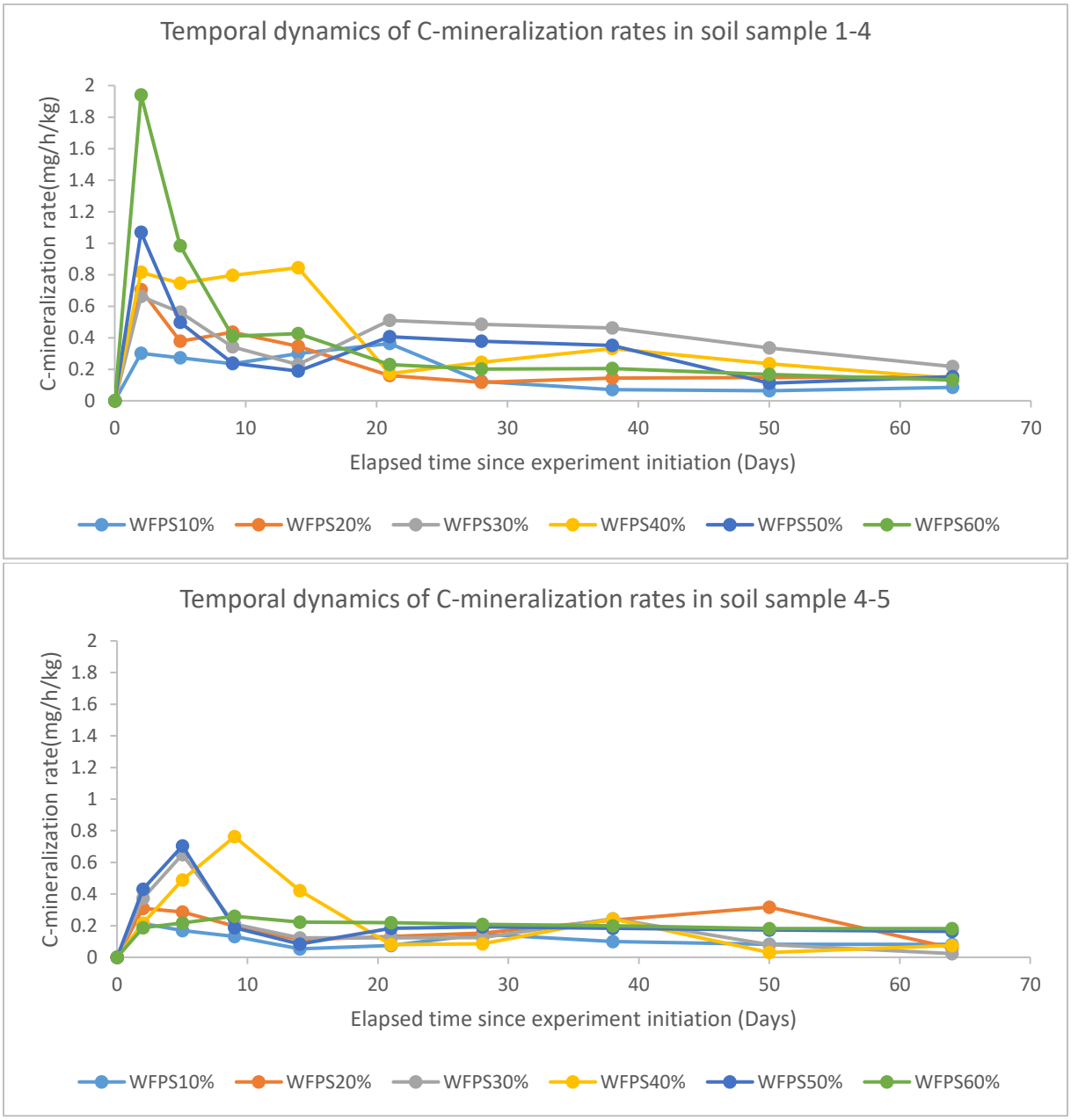

Fig. 9 *Temporal dynamics of C-mineralization rates in soil samples 1-4 and 4-5 across 6 soil moisture levels*

4.1.2 Dynamic evolution of cumulative C- mineralization

Following calculations steps described in session 3.4.5, the cumulative C mineralization rate is derived, quantified as mg/kg of dry soil, representing the accumulated carbon mineralization in mg per kg of soil over time.

Fig.10 portrays this evolution across diverse moisture levels again for samples 1-4 and 4-5. In both soils, cumulative mineralization patterns evolved towards a linear course after an initial exponential decline of the mineralization rate. This pattern suggests indeed that a parallel first and zero order kinetic model would fit well to the data. Patterns for the other 8 soils were comparable.

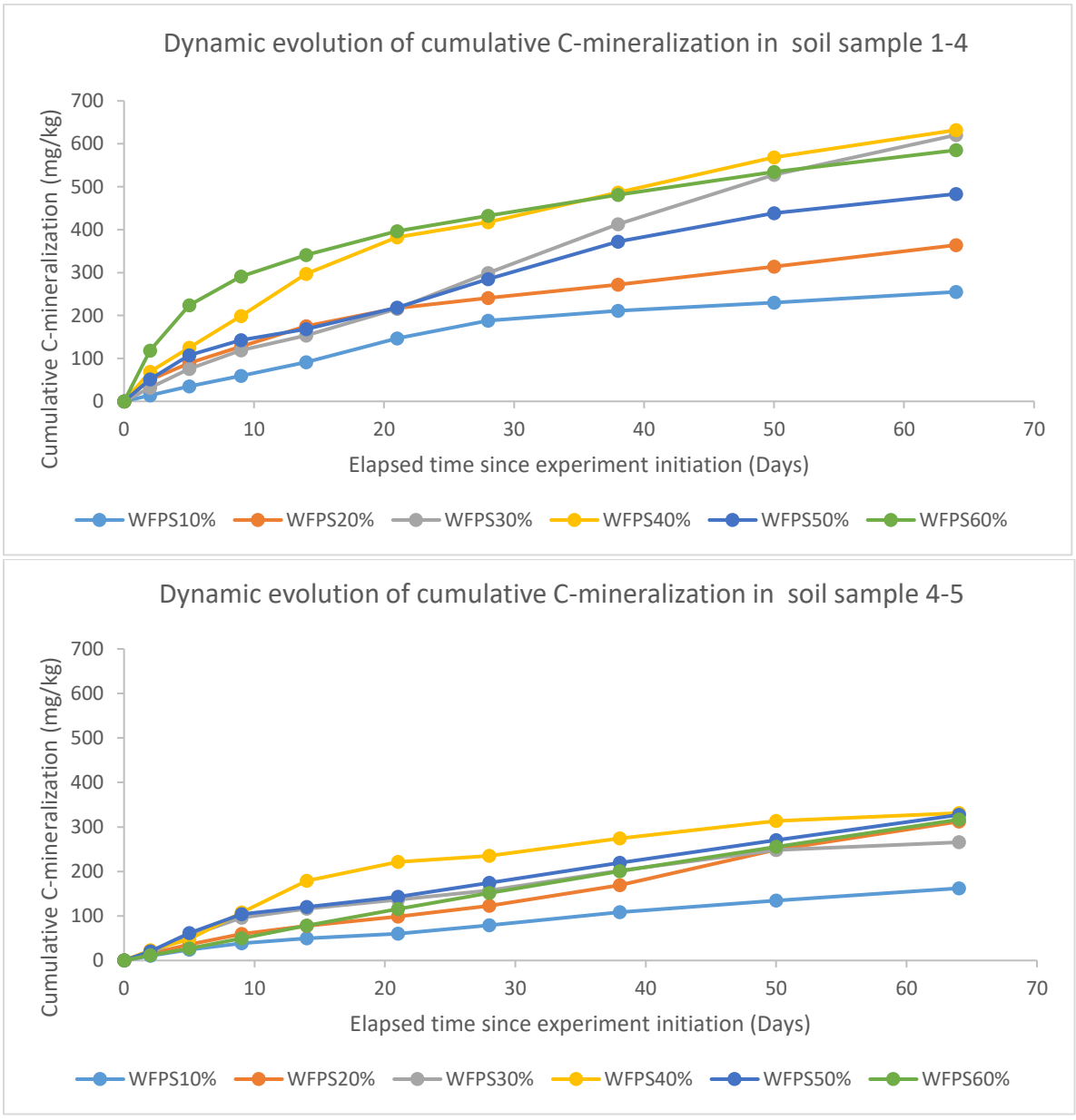

Fig. 10 *Dynamic evolution of the cumulative amount of C mineralized in soil samples 1-4 and 4-5 across 6 soil moisture levels*

4.2 Relative cumulative C-mineralization

The cumulative relative C-mineralization is calculated by dividing the cumulative carbon mineralization by the SOC content of the sample, measured in mg/kg of dry soil. The result is then expressed as mg C/g SOC, representing the quantity of carbon mineralized (in mg) per gram SOC. Fig. 11 illustrates this progression in samples 1-4 and 4-5.

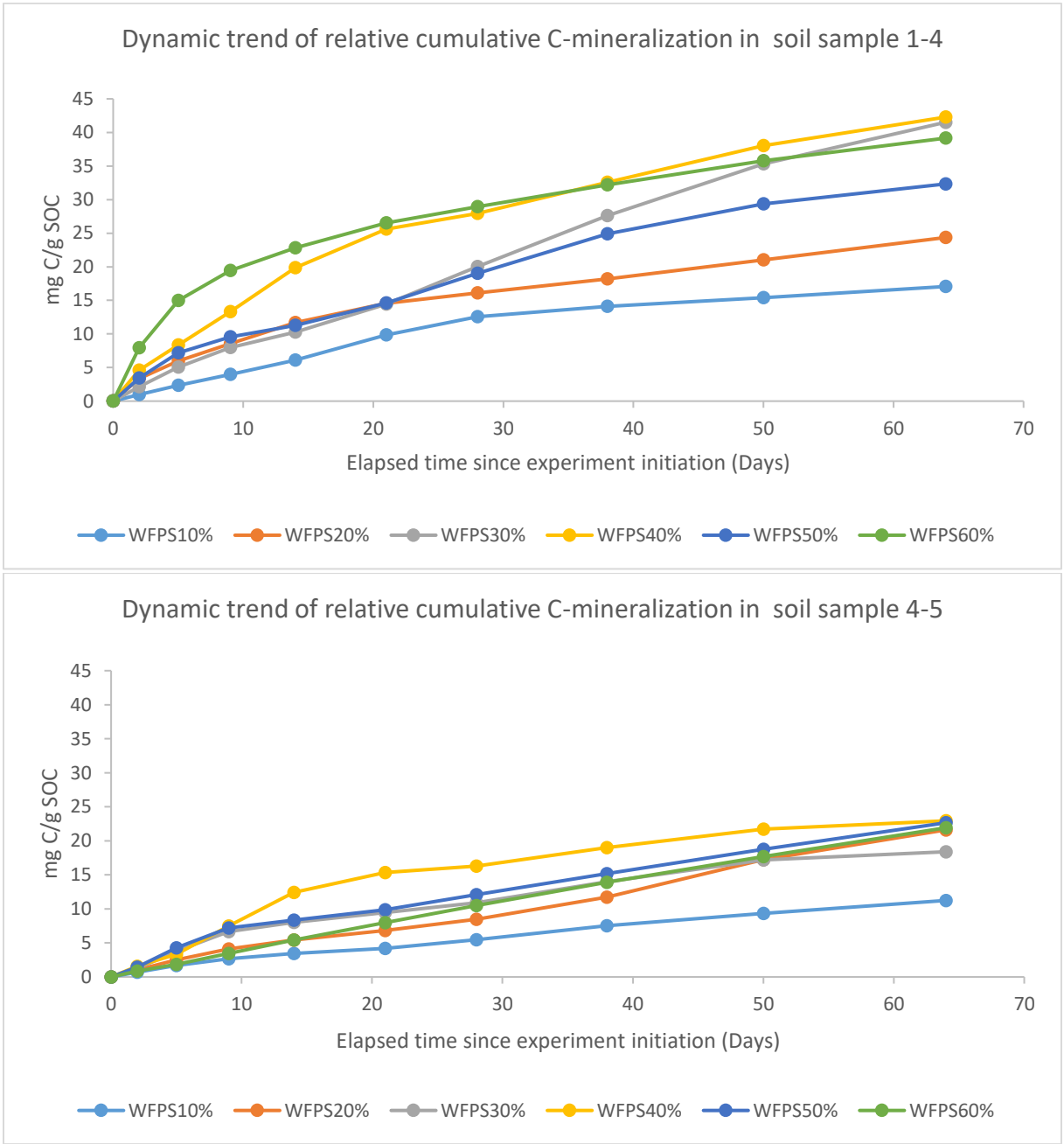

Fig. 11 *Temporal changes in relative cumulative C-mineralization across 6 soil moisture levels in soil samples 1-4 and 4-5*

4.3 Fitting non-linear models to the relative cumulative C-mineralization data and correlation analysis

4.3.1 Fit of non-linear models to the relative cumulative C-mineralization data

As previously mentioned, model fitting and evaluation were conducted using the nlsLM() function in the R programming language for the equation C_rel = ks * Days + Ca * (1-exp(−kf * Days)). The results of fitting this model to the cumulative relative C-mineralization data are outlined in Table 6. This fitting procedure involves determining the optimal parameter values for ks, Ca, and kf that closely correspond to the observed data points. To gauge the adequacy of the fit, we visually compared the predictions of model with the actual data and employed statistical measures like the R^2 and the root mean squared error (RMSE) or normalized root mean squared error (NRMSE).

The fitting results reveals fluctuations in R^2 values across varying WFPS levels, posing challenges in definitively establishing whether higher or lower WFPS levels consistently resulted in enhanced or diminished model fits. Particularly, a clear monotonic trend wherein R^2 systematically increases or decreases with rising WFPS levels is absent, with certain instances showing that higher WFPS levels align with elevated R^2 values, while in contrasting instances, they align with reduced R^2 values.

Initially, assessing the average magnitude of deviations between predicted and observed values through RMSE, we then transitioned to NRMSE. Remarkably, about two-thirds of the NRMSE values demonstrated values below 0.1, with the remaining NRMSE values falling within the range of 0.1 to 0.17. When coupled with the R-squared metrics that the majority of R^2 values surpassed 0.9 and the remaining values exceeded 0.75, this demonstrates that the selected parallel 1st and 0-order kinetic model was well able to describe the temporal course of the cumulative relative C mineralization.

***Table 6**: Parameters for the 0-1 parallel kinetic C mineralization model C_rel = ks * Days + Ca * exp(−kf * Days) fitted to the relative cumulative C-Mineralization data (in mg C / g SOC)*

Soil Sample	WFPS (%)	ks (mg C / g SOC / days)	Ca (g SOC / g SOC)	kf (1/days)	R_squared	RMSE	NRMSE
1-4	10	0.2808	1.7539	-1E-06	0.9188	1.7178	0.1007
1-4	20	0.3636	3.6863	2.18E-06	0.9141	2.2979	0.0943
1-4	30	0.6574	1.2452	-2.7E-07	0.9946	0.9943	0.0240
1-4	40	0.6623	5.5009	7.79E-07	0.9219	3.9767	0.0940
1-4	50	0.4970	3.6896	1.38E-06	0.9659	1.9220	0.0595
1-4	60	0.5595	9.1222	-3.2E-07	0.8298	5.2260	0.1335
2-3	10	0.3827	3.7427	1.62E-08	0.9308	2.1479	0.0825
2-3	20	0.5121	4.3932	-3.7E-06	0.9399	2.6721	0.0783
2-3	30	0.6599	5.7762	-3.8E-08	0.9599	2.7756	0.0611
2-3	40	0.7976	9.4398	4.66E-06	0.9018	5.4287	0.1003
2-3	50	0.6602	5.5626	-4.9E-08	0.9630	2.6634	0.0598
2-3	60	0.8796	13.3058	-9E-07	0.8484	7.6678	0.1267
2-5	10	0.4788	3.3595	2.9E-07	0.9729	1.6457	0.0498
2-5	20	0.6219	8.9806	5.5E-07	0.8521	5.3441	0.1229
2-5	30	0.5928	8.9127	-4.8E-07	0.8824	4.4539	0.1052
2-5	40	0.7621	12.2816	4.46E-06	0.8546	6.4818	0.1182
2-5	50	0.5539	10.8230	7.22E-07	0.8400	4.9752	0.1194
2-5	60	0.8651	11.7613	-1.7E-07	0.8859	6.4035	0.1055
2-8	10	0.6152	-0.8538	-0.03924	0.9898	0.7157	0.0249
2-8	20	0.4578	6.1102	4.4E-07	0.8424	4.0842	0.1337
2-8	30	0.5146	4.6555	-6.1E-08	0.9533	2.3450	0.0686
2-8	40	0.6139	6.5398	-1.6E-06	0.9065	4.0661	0.0958
2-8	50	0.5557	5.9704	-1.8E-07	0.9379	2.9427	0.0770
2-8	60	0.7104	13.2004	-2.3E-07	0.7553	8.3394	0.1651
3-1	10	0.5869	1.5572	1.75E-06	0.9946	0.8912	0.0234
3-1	20	0.7145	7.8840	-8.5E-07	0.9159	4.4651	0.0883
3-1	30	0.6864	6.1047	3.47E-07	0.9643	2.7192	0.0580
3-1	40	0.7384	11.7119	1.02E-07	0.8500	6.3983	0.1218
3-1	50	0.7199	8.4468	-2.5E-07	0.9288	4.1029	0.0832
3-1	60	0.9331	12.4561	-2.8E-07	0.8724	7.3599	0.1159
3-13	10	0.3401	1.8363	3.43E-07	0.9615	1.4014	0.0660
3-13	20	0.3978	4.6861	-2.1E-08	0.9368	2.1309	0.0763
3-13	30	0.5163	4.2708	3.64E-07	0.9659	1.9955	0.0568
3-13	40	0.6760	6.5942	-6.7E-08	0.9480	3.2651	0.0708

3-13	50	0.5582	5.1058	-9.1E-08	0.9606	2.3276	0.0597
3-13	60	0.5710	3.6234	8.99E-07	0.9723	1.9873	0.0537
3-15	10	0.3767	3.4631	-5.1E-07	0.9229	2.2410	0.0915
3-15	20	0.4706	4.6035	1.75E-07	0.9532	2.1504	0.0671
3-15	30	0.5627	4.8837	-4.9E-07	0.9414	2.8882	0.0789
3-15	40	0.7080	6.9094	6.95E-10	0.9219	4.2709	0.0930
3-15	50	0.4712	5.5657	7.17E-07	0.9317	2.6263	0.0803
3-15	60	0.4471	7.5915	3.12E-06	0.8600	3.7195	0.1133
4-2	10	0.3386	2.2110	-1.3E-07	0.9747	1.1233	0.0504
4-2	20	0.4136	4.9405	1.38E-07	0.8692	3.3091	0.1207
4-2	30	0.3338	3.3095	-4.7E-07	0.9526	1.5320	0.0646
4-2	40	0.4143	6.3765	-3.1E-06	0.8828	3.1132	0.1026
4-2	50	0.3670	4.5984	-1.1E-06	0.9210	2.2111	0.0881
4-2	60	0.3018	6.1553	-2.3E-06	0.7878	3.2309	0.1457
4-5	10	0.1715	0.6558	3.12E-06	0.9906	0.3431	0.0305
4-5	20	0.3323	0.4060	0.050876	0.9876	0.6078	0.0281
4-5	30	0.2821	2.4474	1.37E-06	0.9399	1.4697	0.0799
4-5	40	0.3785	2.9885	-5.2E-06	0.8823	2.8511	0.1243
4-5	50	0.3331	2.2845	-4.1E-08	0.9693	1.2201	0.0539
4-5	60	0.3478	0.2840	-9.1E-07	0.9978	0.3373	0.0154
4-8	10	0.3121	3.3050	7.63E-07	0.9344	1.7014	0.0792
4-8	20	0.3443	4.9079	-4.4E-07	0.8646	2.8106	0.1183
4-8	30	0.4121	4.1873	4.25E-06	0.9340	2.2550	0.0814
4-8	40	0.3649	5.7535	-2.2E-07	0.8810	2.7665	0.1051
4-8	50	0.4496	5.6942	-2.1E-07	0.9047	3.0025	0.0971
4-8	60	0.4481	7.8391	-1.9E-06	0.8261	4.2402	0.1322

4.3.2 Correlation between SOC properties, and the C-mineralization model parameters in cumulative relative C-mineralization

Using Pearson correlation test, we calculated correlation coefficients between TOC, and relative shares of POM, MAOM, DOC, and the three model parameters — ks, Ca, and kf — from formula rel cumulative C-min = ks * Days + Ca * exp(−kf * Days). In addition the soil moisture content (expressed in terms of %WFPS) was also included. The outcomes of this analysis are presented in Table 7.

***Table 7**: Correlation coefficients between key factors and parameters of the fitted C-mineralization model (* and ** indicate significant correlations at $p<0.05$ and $p<0.01$, respectively)*

	ks	Ca	kf
WFPS	0.3895**	0.5468 **	0.0256
TOC	-0.3669**	-0.3819**	0.1610
Relative share of POM	-0.0044	-0.1628	0.2671*
Relative share of MAOM	-0.0054	0.1522	-0.2665 *
Relative share of DOC	0.2685 *	0.3119*	-0.0585

In Table 7, among the statistically significant correlations, WFPS exhibits a moderate positive correlation with ks and Ca, while showing no correlation with kf. As for TOC, moderate negative correlations are observed with both ks and Ca, without any significant correlation with kf. Neither POM nor MAOM show linear correlations with ks and Ca. However, a subtle positive correlation is discerned between POM and kf, accompanied by a similarly weak negative correlation between MAOM and kf. Regarding DOC, faint positive correlations are identified with ks and Ca, yet no significant linear correlation is observed with kf.

4.4 Exploring the interplay of % WFPS and POM on C-mineralization dynamics using a Gaussian function

4.4.1 Exploring the interplay between relative cumulative C-mineralization and % WFPS using Gaussian function

Gaussian models were used to mathematically describe the relation between the predicted relative cumulative carbon mineralization at DAY = 60 obtained from the fitted non-linear C-mineralization models, and the water-filled pore space (WFPS) percentage.

Fig. 12 presents the results and quality of fit for a Gaussian function applied to soil samples 1-4 and 4-5. The Gaussian model parameters optimal relative carbon release rate, intrinsic Gaussian function parameter (ξ), actual soil moisture (%WFPS), and optimal moisture (%WFPS_opt) are indicated as well. And Table 9 below showcases the Gaussian function parametrization and fit for all 10 soils.

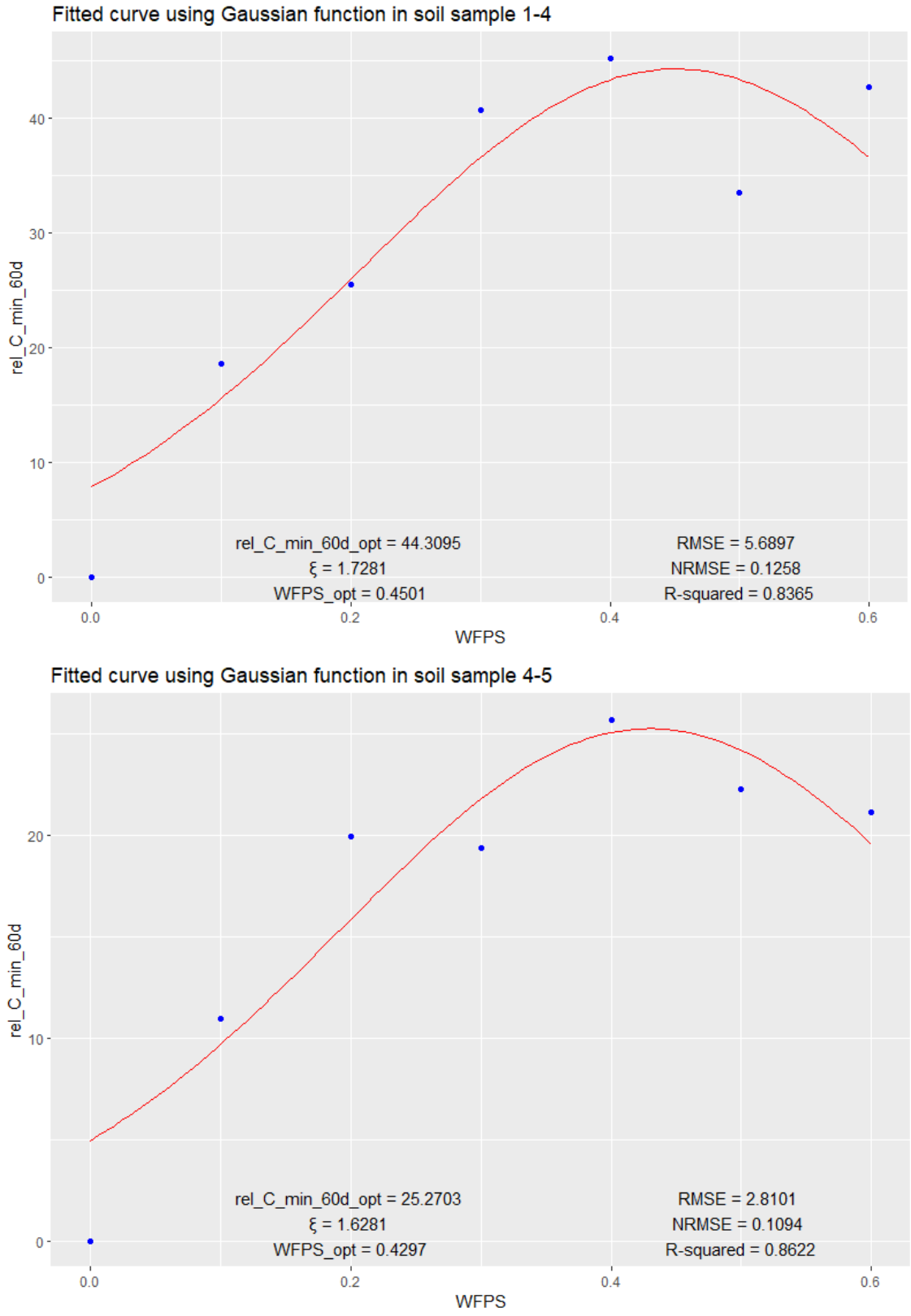

Fig. 12 *Gaussian function fitting of relative cumulative C-mineralization with WFPS in soil samples 1-4 and 4-5*

***Table 8**: Outcomes illustrating the dependency of the relative cumulative C-mineralization and %WFPS using Gaussian function*

Soil Sample	%WFPS_opt	ξ	rel_C_min_60d_opt (mg C /g SOC)	R^2	RMSE	NRMSE
1-4	45.01%	1.7281	44.3	0.8365	5.6897	0.1258
2-3	54.89%	1.5627	59.6	0.8182	8.1345	0.1231
2-5	50.11%	1.3017	58.0	0.7051	9.8577	0.1548
2-8	60.74%	1.3417	50.4	0.7616	7.4381	0.1332
3-1	52.87%	1.2350	62.2	0.7103	10.2219	0.1493
3-13	43.67%	1.6874	44.6	0.8842	4.5905	0.0973
3-15	39.45%	1.5401	45.4	0.8104	5.7992	0.1174
4-2	38.90%	1.1672	31.0	0.6245	5.5098	0.1764
4-5	42.97%	1.6281	25.3	0.8622	2.8101	0.1094
4-8	49.93%	1.2383	34.0	0.7394	5.1576	0.1485
Average	47.85%	1.4430	45.5			
Standard Deviation	7.07%	0.2083	12.5			

From Table 8, in the preliminary NRMSE assessment, it is worth highlighting that the vast majority of NRMSE values stayed below 0.17. Moreover, upon examining the R^2 metric, five numerical R^2 values surpassed 0.8, while four fell between the range of 0.7 and 0.8. Only one exception was observed, at 0.62. This demonstrates that the final model attained a relatively acceptable level of accuracy for most soils.

Among the 10 soil samples analyzed, the optimal conditions for C-mineralization were observed at an average WFPS_opt of 47.85%, with a moderate level of variability indicated by a standard deviation of just 7.07%. The average value for ξ is 1.4403, showing relatively consistent behavior, and its standard deviation is 0.2083

The rel_C_min_60d_opt, which signifies the relative amount of SOC mineralized at optimal moisture level had an average of 45.5 mg C / g SOC, while its standard deviation is higher at 12.5, indicating a notable variability in this parameter among the samples. This also signifies that about 4.5% of SOC got mineralized during the course of the 60-days incubation period.

4.4.2 Results for correlation analysis of key factors and parameters of Gaussian function

Using Pearson correlation test, we calculated correlation coefficients between the TOC, relative shares of POM, relative shares of MAOM, relative shares of DOC, and the three model parameters — %WFPS_opt, ξ and rel_C_min_60d_opt (% of SOC mineralized) from fitted Gaussian function. The outcomes of this analysis are presented in Table 9.

By plotting the relative proportion of POM to parameters of fitted Gaussian function we illustrated the influence of POM fraction fluctuations on shifts in rel_C_min_60d_opt (% of SOC mineralized), %WFPS_opt, and ξ, shown in Fig. 13.

***Table 9**: Correlation coefficients between key factors and the fitted parameters of Gaussian function (* and ** indicate significant correlations at p<0.05 and p<0.01, respectively)*

	%WFPS_opt	**ξ**	**rel_C_min_60d_opt (mg C /g SOC)**
TOC	-0.5582 *(p<0.1)*	0.5142	-0.4433
Relative share of POM	0.0430	0.2956	-0.0552
Relative share of MAOM	-0.0498	-0.2740	0.0441
Relative share of DOC	0.1786	-0.6310 *(p<0.1)*	0.3093

In Table 9, some correlations among the variables are discernible at a less stringent significance threshold ($p < 0.1$). Notably, a marginal negative correlation emerges between TOC and %WFPS_opt, implying that as TOC rises, %WFPS_opt tends to decline. Additionally, there was a moderate negative correlation between the relative share of DOC and ξ. However, no significant correlations are observed among the remaining variables.

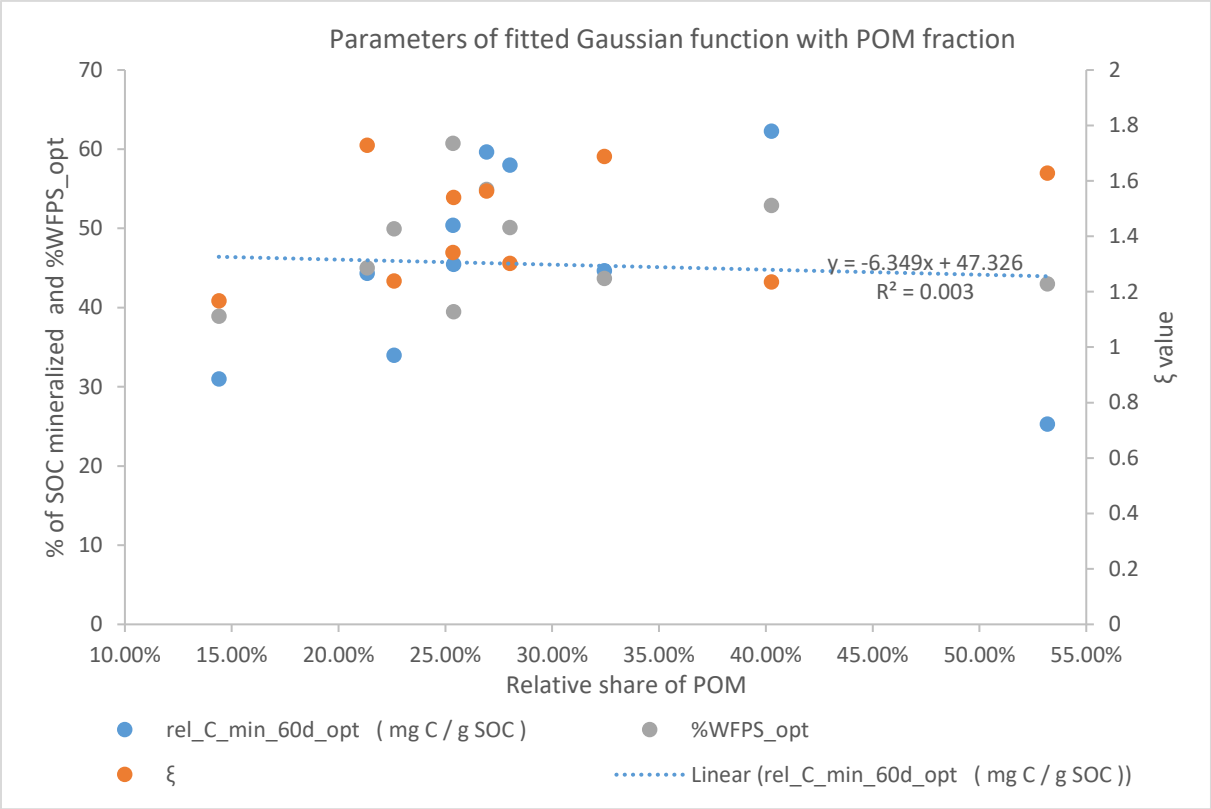

Fig. 13 *Influence of POM fraction fluctuations on parameters of fitted Gaussian function across ten soil samples*

4.4.3 Correlation analysis results for key Factors and parameters of Gaussian function excluding one data point with unusually high POM content

One of the 10 soils had an exceptionally high POM content, which is highly unusual for cropland soils. The relation with the cumulative relative amount of C mineralized deviated also. After removing this data point with high POM content, we once more calculated correlation coefficients between TOC, POM, MAOM, DOC, and three model parameters (%WFPS_opt, ξ, and rel_C_min_60d_opt) from the Gaussian function. Results are in Table 10. We then connected relative POM shares to Gaussian function parameters to show how POM fluctuations influence shifts in rel_C_min_60d_opt, %WFPS_opt, and ξ, as seen in Figure 14.

***Table 10**: Correlation coefficients between key factors and the fitted parameters of Gaussian function excluding one data point with unusually high POM content and deviating relative mineralization (* and ** indicate significant correlations at p<0.05 and p<0.01, respectively)*

	%WFPS_opt	ξ	rel_C_min_60d_opt (mg C /g SOC)
TOC	-0.5208	0.4550	-0.3174
Relative share of POM	0.3829	0.0875	0.7505*
Relative share of MAOM	-0.3810	-0.0560	-0.7428*
Relative share of DOC	0.0847	-0.5791	0.0880

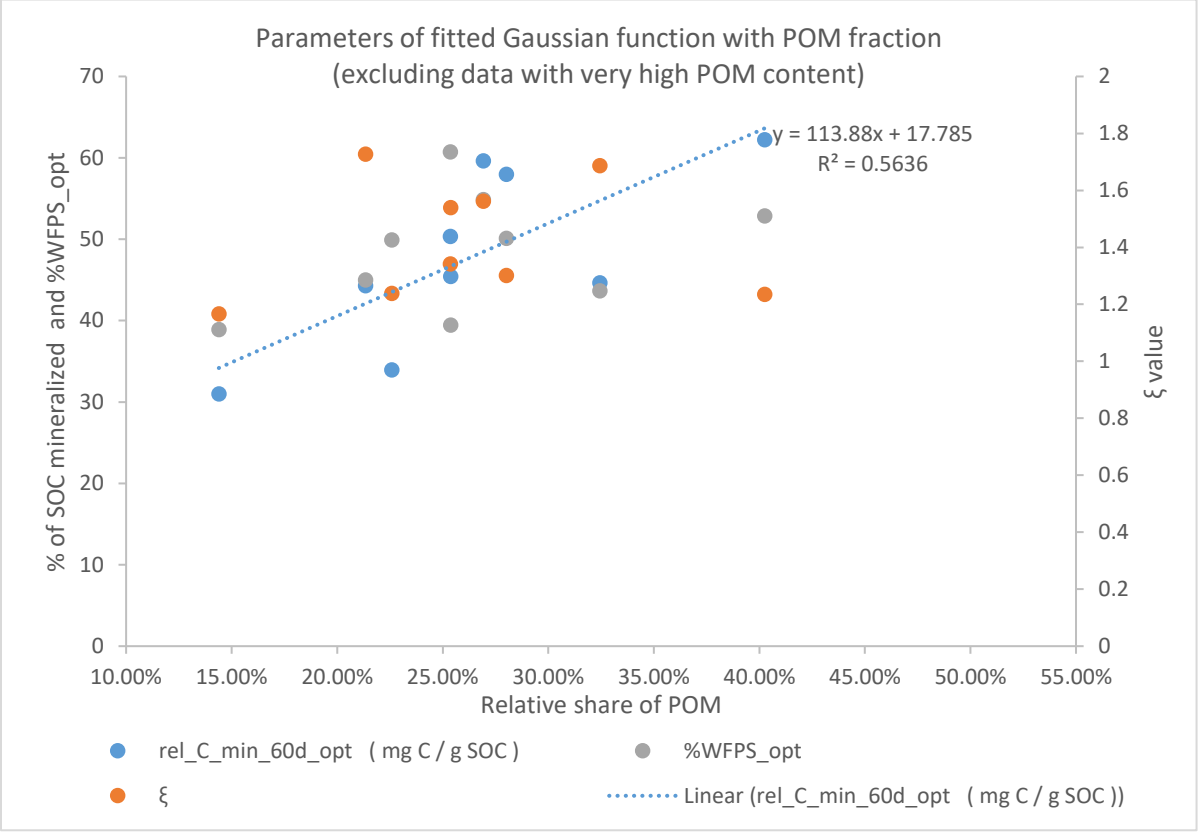

***Fig. 14** Influence of POM fraction fluctuations on parameters of fitted Gaussian function across ten soil samples (excluding one data point with unusually high POM content)*

Table 10 reveals several statistically significant correlations at the $p < 0.05$ level. Notably, the fitted parameter rel_C_min_60d_opt exhibited a strong positive correlation with the relative share of POM and a robust negative correlation with the relative share of MAOM. However, no significant correlations are observed among the Gaussian function model parameters and SOM fraction proportions as when all soils were included in the analysis.

5. DISCUSSION

5.1 Dynamics of C-Mineralization

5.1.1 Dynamics of C-Mineralization rates

The data depicted within Fig. 9 provides a typical insight into the progress of SOC mineralization after soil rewetting, as was done artificially in the lab in our incubation experiment. The observed temporal trends are characterized by an initial sharp ascent in carbon mineralization, which is succeeded by a progressive attenuation towards a stabilization of the SOC mineralization rates.

In our laboratory environment, we exposed soil samples to arid dry treatments, resulting in the disruption of the original soil structure. Throughout the experiment, the soil underwent compression to establish uniform porosity and was deliberately selected to closely resemble a consistent soil texture. And we introduced water to the air-dried soil samples, essentially and effectively simulating soil rewetting. Following the rewetting process, observed across diverse laboratory and ecological drought scenarios, there was a notable and consistent rise in carbon dioxide flux. This phenomenon has been extensively documented in numerous scientific publications (Kim et al., 2012; Song et al., 2017). Rewetting dry soils is associated with a burst of microbial activity and mineralization, which manifests itself as a pulse in soil CO_2 emissions, long-known as the Birch effect (Barnard et al., 2020). Such microbial growth in response to simulated rewetting is nearly always rapid (Song et al., 2017) and arises from a mix of abiotic and biotic sources, with significant contributions from compatible solutes, microbial necromass, altered water film connectivity, sustained extracellular enzyme activity, mineral surface C desorption, and aggregate disruption; notably, in low carbonate soils, biotic mechanisms largely outpace abiotic ones in driving the post-rewetting CO_2 pulse (Barnard et al., 2020). After several weeks the C mineralization rates lowered and stabilized, likely owing to depletion of easily mineralizable C, with then further slower microbially mediated mineralization of more stable or less accessible SOC.

5.1.2 Dynamic evolution of cumulative C-mineralization and the relative cumulative C-mineralization

Cumulative C mineralization pertains to the total amount of carbon that has undergone mineralization, while relative cumulative carbon mineralization entails dividing the

cumulative C mineralization by the total organic carbon, allowing for the utilization of this ratio in expressing normalized mineralized C based on the unit mass of organic C. The temporal trends in their carbon mineralization dynamics, as illustrated in Figs. 10 and 11, indicate a shared variation pattern. Initially, both metrics exhibit a distinct and robust upward pattern, reflecting the heightened metabolic activity of microorganisms following the introduction of water. This trend underscores the accelerated breakdown of organic matter, resulting in the subsequent release of carbon compounds into the surrounding environment, as depicted in 5.1.1. As time progresses, the once steep incline in both cumulative C-mineralization and relative cumulative C-mineralization gradually evolves into a more subdued and consistent growth trajectory. This transition toward a steadier accumulation rate signifies a maturation or equilibrium within the mineralization process. This phenomenon has been documented in numerous sources, although there are variations in the specific treatments employed, and it implies that the initial surge in microbial activity and carbon mineralization, driven by increased moisture and its associated factors, gets progressively moderated, potentially due to regulatory mechanisms or limitations in substrate availability (Barnard et al., 2020; Guo et al., 2019; Kaur et al., 2023; Liyanage et al., 2021; Sawada et al., 2016).

With the correlation to increased substrate availability and a larger microbial biomass in soils with higher SOC, expressing respiration data based on the unit mass of organic C is advisable to mitigate the impact of organic C on the respiration process. (Butterly et al., 2010; Sawada et al., 2016). The relative cumulative C-mineralization data was accordingly organized in this unit format and utilized for fitting the parallel first- and zero-order kinetic model. This model was well able to capture the progression of the cumulative C mineralization: i.e. a first exponential course was followed by further linear progression of the cumulative C mineralization.

5.2 Exploring Kinetics of relative cumulative C-mineralization by examining correlation coefficients between the key factors and parameters of the fitted model

Upon scrutinizing correlation coefficients between the soil factors and parameters of the kinetic C-mineralization model, the following observations come to light:

WFPS demonstrates a positive correlation ($p<0.01$) with both Ca and ks, implying that within a certain range, as WFPS increases, the easily degradable carbon pool and the mineralization rate of the resistant carbon also tend to rise. This could be attributed to improved solute movement, increased microbial activity, and better nutrient availability in more moist conditions (Moyano et al., 2013). Such was obviously expected as our study specifically targeted the dry end of the WFPS – soil respiration bell curve, for which indeed a positive monotonic (but not necessarily linear) relation is expected.

TOC has a moderate negative correlation with Ca and ks ($p<0.01$), indicating that elevated levels of total organic carbon are linked to a decrease in the easily degradable carbon pool and lower mineralization rates of the resistant carbon pool. This pattern could be attributed to that higher SOC was associated with an abundance of lignin, polysaccharides and n-alkanes, whereas lower SOC was related to an abundance of unsaturated fatty acids and less-stabilized SOM (Yang et al., 2022). Likewise observations for sandy soils in NW-Europe had been made: specific land-use history of forest and heathland tend to accumulate recalcitrant SOM in sandy croplands(Springob & Kirchmann, 2003). Possibly that likewise explanation was also valid for the current investigated set of light textured soils.

The **relative share of POM** exhibited a positive correlation with kf as supported by the correlation coefficient of 0.2671, while the **relative share of MAOM** demonstrates a negative correlation with kf as indicated by the correlation coefficient of -0.2665). As TOC is primarily partitioned into POM and MAOM with minimal DOC contribution, this leads to inverse relationships between the percentages of POM and MAOM. When one is correlated with a parameter and exhibits a correlation coefficient, the other will naturally demonstrate a similar but opposite correlation coefficient due to their mathematical complementarity. Their correlation coefficients suggest that with an increase in the proportion of POM in the soil or a decrease in the proportion of MAOM, the **kf** tends to rise, indicating that higher POM content and lower MAOM content is associated with the higher mineralization rate constant of the easily degradable carbon pool. This variation may logically stem from their

inherent characteristics, where POM remains largely unbound in the soil matrix, while the formation of MAOM occurs through chemical interactions with mineral surfaces, resulting in reduced accessibility for decomposers (Just et al., 2023b; Mirabito & Chambers, 2023b) .

The **relative share of POM or MAOM** did not display any correlation with **ks and Ca**, suggesting that the easily degradable carbon pool and mineralization rate constant of the resistant pool are not linked to the varying shares of POM or MAOM within the total organic carbon content. This phenomenon can be elucidated as follows: (1) Initially, there is a clear and strong upward trend in Cumulative C mineralization or relative cumulative carbon mineralization, attributed to the CO_2 pulse (following soil rewetting) that arises from a combination of abiotic and biotic sources, including compatible solutes, microbial necromass, modified water film connectivity, persistent extracellular enzyme activity, mineral surface C desorption, and aggregate disruption (Barnard et al., 2020). So, in this model, Ca parameter, the easily degradable carbon pool may be related to the most prevalent sources and mechanisms that fuel the C mineralization pulse. (2) The relative share of POM or MAOM might relate to the resistant soil pool, but it does not seem to connect with its mineralization rate constant. Instead, other factors like soil nutrient availability, WFPS, pH and soil structure might be more likely to influence this rate constant. Indeed the persistence of SOC in soil has been advocated not to be so much the resultant of intrinsic biochemical stability of the SOM, but rather derives from ecological impediments to the soil microbial community.

Lastly, the **relative share of DOC** had a moderate positive correlation ($p<0.05$) with **ks and Ca**. While dissolved organic matter (DOM) is commonly thought of as the more labile fraction of soil organic matter with minimal contribution to soil carbon accumulation, recent research challenges this perspective by highlighting that aromatic compounds originating from lignin are likely the more persistent constituents of DOM, whereas plant-derived carbohydrates appear to undergo easier degradation (Kalbitz & Kaiser, 2008). Our fitting results additionally substantiate this assertion.

5.3 Correlation analysis of key factors and parameters fitted Gaussian function parameters in the context of relative cumulative C-mineralization dependency on WFPS

Using R^2 and NRMSE to assess the fit of the Gaussian function model, the results strongly indicate a good to high level of accuracy in the fitting. Through the fitted Gaussian function model, the parameters $rel\ C_{min-60d;opt}$, ξ and $\%WFPS_{opt}$ were determined, followed by linking these fitted parameters to critical factors including TOC, and the relative distribution of POM, MAOM, and DOC .

In our all-inclusive analysis, results (Table 9) consistently show no significant linear relationships among variables at $p < 0.05$, while at $p < 0.1$, some associations emerge, including a moderate negative correlation between TOC and %WFPS_opt, as well as a similar correlation between the relative DOC proportion and the ξ parameter. These results essentially point at but a limited dependency of the Rh – WFPS relation onto SOM quality, **in contrast to our hypothesis**. We expected that with higher POM content, the Rh dependency on %WFPS would increase, as POM resides in a coarser share of the soil pore space that is either water or air filled much depending on WFPS, while smaller MAOM resides in permanently moist smaller pores, regardless of %WFPS in the investigated range. Apparently, this reasoning was not correct and ecological relations between SOM quality and soil moisture are more complex.

Upon excluding one data point with a high POM content and deviating apparent stability of the SOC, significant correlations ($p < 0.05$) did emerge between rel_C_min_60d_opt and relative share of POM or MAOM (Table 10). This to the least underscores a rather complex link between the optimal C mineralization rate at the ideal %WFPS and both the POM and MAOM fractions, that are intricately intertwined with the inherent properties of POM and MAOM (Lavallee et al., 2020). But when the high POM soil was included this relation was lost. Considering about all the data, the origin of this phenomenon seems to be connected to the impact of a POM fraction that bears resemblance to soil moisture on respiration rates (Rh rates), but then in an opposite direction: The relative cumulative C-mineralization might exhibit a non-monotonic response to POM content with dips at the lowest and highest POM fraction extremes, while reaching its highest point at a specific level of POM. Is there a particular POM fraction that corresponds to the highest level of relative cumulative C-mineralization? Currently, the available literature does not provide direct evidence to support this concept. However, in some studies, it was found that higher POM

concentrations, such as in no-till systems, these were linked to increased nonmineralizability of SOC, as indicated by relative cumulative C-mineralization in this thesis, compared to tillage practices (Dimassi et al., 2014). In another study, a negative correlation was observed between C relative C- mineralization and POC concentration (Kan et al., 2020), and this opposing trend could be clarified by the concept of physical protection enabled through aggregation, where the existence of POC contributes to macro-aggregate formation, reinforces aggregate stability, and thereby shields SOC from mineralization (Kan et al., 2020; Six et al., 2002). Likewise as explained above in NW-European sandy soils high SOM levels (and POM levels) can be associated with former land-use leading to accumulation of stable SOM (Springob & Kirchmann, 2003). Such unexplained variation in SOM recalcitrance may have distorted examined relations between %WFPS and Rh in this study as well. A further analysis of the biochemical quality and land-use history of the current soil set would aid in clarifying this.

6. CONCLUSION

The primary findings of the thesis encompass several essential aspects: firstly, an observed rapid escalation in carbon mineralization immediately after soil rewetting, validating the Birch effect; secondly, consistent temporal trends in both cumulative carbon mineralization and relative cumulative carbon mineralization, demonstrating an initial steep rise followed by a stabilization phase, indicating a transition toward a more balanced mineralization process. Thirdly, through correlation analysis, the study underscores the influence of diverse factors on mineralization rates, particularly highlighting the moderate positive correlation between soil moisture (measured as WFPS) and both the easily degradable carbon pool (Ca) and the mineralization rate constant of resistant carbon (ks), while revealing a negative correlation between total organic carbon (TOC) and both Ca and ks, suggesting the intricate role of organic carbon composition in governing mineralization dynamics. Fourth, the investigation of organic matter fractions reveals the notable role of particulate organic matter (POM) and mineral-associated organic matter (MAOM) fractions, with correlations observed between their relative shares and the mineralization rate constant (kf), where higher POM content and lower MAOM content are linked to heightened mineralization rates, emphasizing their distinct contributions to carbon turnover.

Finally and most importantly, employing a Gaussian function model to describe WFPS C-mineralization relations and further correlation analysis of model parameters and SOM fractions did not unveil significant correlations. Thereby our primary hypothesis was refuted: with increasing POM proportion there was no stronger dependency of relative C mineralization on %WFPS. We could thus not directly identify SOM quality, at least when expressed in terms of POM and MAOM proportions, as key determinant of the WFPS – Rh relation. When excluding one data point with unusually stable SOM and high POM content, there were relations between optimal C mineralization rates, soil moisture, and the DOM proportion. But again that result did not suggest a substantial mediation of the WFPS – Rh relation by POM or MAOM proportion, contrary to our hypothesis.

However, it is imperative to acknowledge the constraints imposed by the reliance of study on controlled laboratory conditions and fitting models, which may not comprehensively encapsulate the intricacies inherent to real-world field environments. While correlations have been discerned, the underlying mechanisms warrant further elucidation. One important aspect was the short duration of the carried out incubations, viz. 60 days, which may well prove too limited to accurately describe kinetics of the more stable SOM pools, which by far constitute the largest part of SOM. At time of compiling this thesis the experiments were still running and perhaps with further collected C-mineralization data a

more robust analysis of stable C-pool mineralization kinetic - %WFPS dependency onto SOM quality could yet be investigated.

7. REFERENCES

Barnard, R. L., Blazewicz, S. J. & Firestone, M. K. (2020). Rewetting of soil: Revisiting the origin of soil CO2 emissions. *Soil Biology and Biochemistry*, *147*, 107819. https://doi.org/10.1016/j.soilbio.2020.107819

Bernoux, M. & Cerri, C. E. P. (2005). Encyclopedia of Analytical Science (Second Edition). *Article Titles: G, Organic Geochemistry312000*, 203–208. https://doi.org/10.1016/b0-12-369397-7/00245-4

Bolan, N. S., Adriano, D. C., Kunhikrishnan, A., James, T., McDowell, R. & Senesi, N. (2011). Chapter One Dissolved Organic Matter Biogeochemistry, Dynamics, and Environmental Significance in Soils. *Advances in Agronomy*, *110*, 1–75. https://doi.org/10.1016/b978-0-12-385531-2.00001-3

Bond-Lamberty, B., Wang, C. & Gower, S. T. (2004). A global relationship between the heterotrophic and autotrophic components of soil respiration? *Global Change Biology*, *10*(10), 1756–1766. https://doi.org/10.1111/j.1365-2486.2004.00816.x

Bosatta, E. & Ågren, G. I. (1999). Soil organic matter quality interpreted thermodynamically. *Soil Biology and Biochemistry*, *31*(13), 1889–1891. https://doi.org/10.1016/s0038-0717(99)00105-4

Bossio, D. A., Cook-Patton, S. C., Ellis, P. W., Fargione, J., Sanderman, J., Smith, P., Wood, S., Zomer, R. J., Unger, M. von, Emmer, I. M. & Griscom, B. W. (2020). The role of soil carbon in natural climate solutions. *Nature Sustainability*, *3*(5), 391–398. https://doi.org/10.1038/s41893-020-0491-z

Butterly, C. R., Marschner, P., McNeill, A. M. & Baldock, J. A. (2010). Rewetting CO2 pulses in Australian agricultural soils and the influence of soil properties. *Biology and Fertility of Soils*, *46*(7), 739–753. https://doi.org/10.1007/s00374-010-0481-9

Calvin, K., Dasgupta, D., Krinner, G., Mukherji, A., Thorne, P. W., Trisos, C., Romero, J., Aldunce, P., Barrett, K., Blanco, G., Cheung, W. W. L., Connors, S., Denton, F., Diongue-Niang, A., Dodman, D., Garschagen, M., Geden, O., Hayward, B., Jones, C., … Connors, S. L. (2023). *IPCC, 2023: Climate Change 2023: Synthesis Report, Summary for Policymakers. Contribution of Working Groups I, II and III to the Sixth Assessment Report of the Intergovernmental Panel on Climate Change [Core Writing Team, H. Lee and J. Romero (eds.)]. IPCC, Geneva, Switzerland.* 1–34. https://doi.org/10.59327/ipcc/ar6-9789291691647.001

Chen, T., Hong, X.-M., Hu, Y.-L., Wang, Q.-K., Yu, L.-Z. & Wang, X.-W. (2022). Effects of litter input on the balance of new and old soil organic carbon under natural forests along a

climatic gradient in China. *Biogeochemistry*, *160*(3), 409–421. https://doi.org/10.1007/s10533-022-00970-4

Cotrufo, M. F. & Lavallee, J. M. (2021). Soil organic matter formation, persistence, and functioning: A synthesis of current understanding to inform its conservation and regeneration. *Advances in Agronomy*, 1–66. https://doi.org/10.1016/bs.agron.2021.11.002

Davidson, E. A. & Janssens, I. A. (2006). Temperature sensitivity of soil carbon decomposition and feedbacks to climate change. *Nature*, *440*(7081), 165–173. https://doi.org/10.1038/nature04514

Dimassi, B., Mary, B., Fontaine, S., Perveen, N., Revaillot, S. & Cohan, J.-P. (2014). Effect of nutrients availability and long-term tillage on priming effect and soil C mineralization. *Soil Biology and Biochemistry*, *78*, 332–339. https://doi.org/10.1016/j.soilbio.2014.07.016

Epron, D. (2009). *Soil Carbon Dynamics*. 157–168. https://doi.org/10.1017/cbo9780511711794.009

Godbold, D. L., Hoosbeek, M. R., Lukac, M., Cotrufo, M. F., Janssens, I. A., Ceulemans, R., Polle, A., Velthorst, E. J., Scarascia-Mugnozza, G., Angelis, P. D., Miglietta, F. & Peressotti, A. (2006). Mycorrhizal Hyphal Turnover as a Dominant Process for Carbon Input into Soil Organic Matter. *Plant and Soil*, *281*(1–2), 15–24. https://doi.org/10.1007/s11104-005-3701-6

Guan, X., Jiang, J., Jing, X., Feng, W., Luo, Z., Wang, Y., Xu, X. & Luo, Y. (2022). Optimizing duration of incubation experiments for understanding soil carbon decomposition. *Geoderma*, *428*, 116225. https://doi.org/10.1016/j.geoderma.2022.116225

Guo, Z., Han, J., Xu, Y., Lu, Y., Shi, C., Ge, L., Cao, T. & Li, J. (2019). The mineralization characteristics of organic carbon and particle composition analysis in reconstructed soil with different proportions of soft rock and sand. *PeerJ*, *7*, e7707. https://doi.org/10.7717/peerj.7707

Hoffland, E., Kuyper, T. W., Comans, R. N. J. & Creamer, R. E. (2020). Eco-functionality of organic matter in soils. *Plant and Soil*, *455*(1–2), 1–22. https://doi.org/10.1007/s11104-020-04651-9

Ikkonen, E. N., García-Calderón, N. E., Stephan-Otto, E., Fuentes-Romero, E., Ibáñez-Huerta, A. & Krasilnikov, P. V. (2020). Soil contribution to CO2 fluxes in Chinampa ecosystems, Mexico. *Spanish Journal of Soil Science*, *10*. https://doi.org/10.3232/sjss.2020.v10.n2.04

Islam, Md. R., Singh, B. & Dijkstra, F. A. (2022). Stabilisation of soil organic matter: interactions between clay and microbes. *Biogeochemistry*, *160*(2), 145–158. https://doi.org/10.1007/s10533-022-00956-2

Just, C., Armbruster, M., Barkusky, D., Baumecker, M., Diepolder, M., Döring, T. F., Heigl, L., Honermeier, B., Jate, M., Merbach, I., Rusch, C., Schubert, D., Schulz, F., Schweitzer, K., Seidel, S., Sommer, M., Spiegel, H., Thumm, U., Urbatzka, P., … Wiesmeier, M. (2023a). Soil organic carbon sequestration in agricultural long-term field experiments as derived from particulate and mineral-associated organic matter. *Geoderma*, *434*, 116472. https://doi.org/10.1016/j.geoderma.2023.116472

Just, C., Armbruster, M., Barkusky, D., Baumecker, M., Diepolder, M., Döring, T. F., Heigl, L., Honermeier, B., Jate, M., Merbach, I., Rusch, C., Schubert, D., Schulz, F., Schweitzer, K., Seidel, S., Sommer, M., Spiegel, H., Thumm, U., Urbatzka, P., … Wiesmeier, M. (2023b). Soil organic carbon sequestration in agricultural long-term field experiments as derived from particulate and mineral-associated organic matter. *Geoderma*, *434*, 116472. https://doi.org/10.1016/j.geoderma.2023.116472

Kalbitz, K. & Kaiser, K. (2008). Contribution of dissolved organic matter to carbon storage in forest mineral soils. *Journal of Plant Nutrition and Soil Science*, *171*(1), 52–60. https://doi.org/10.1002/jpln.200700043

Kan, Z.-R., Virk, A. L., He, C., Liu, Q.-Y., Qi, J.-Y., Dang, Y. P., Zhao, X. & Zhang, H.-L. (2020). Characteristics of carbon mineralization and accumulation under long-term conservation tillage. *CATENA*, *193*, 104636. https://doi.org/10.1016/j.catena.2020.104636

Kaur, H., Kommalapati, R. R. & Saroa, G. S. (2023). Kinetics of native and added carbon mineralization on incubating at different soil and moisture conditions in Typic Ustochrepts and Typic Halustalf. *International Soil and Water Conservation Research*, *11*(2), 365–381. https://doi.org/10.1016/j.iswcr.2023.01.006

Kim, D.-G., Vargas, R., Bond-Lamberty, B. & Turetsky, M. R. (2012). Effects of soil rewetting and thawing on soil gas fluxes: a review of current literature and suggestions for future research. *Biogeosciences*, *9*(7), 2459–2483. https://doi.org/10.5194/bg-9-2459-2012

King, A. E., Ali, G. A., Gillespie, A. W. & Wagner-Riddle, C. (2020). Soil Organic Matter as Catalyst of Crop Resource Capture. *Frontiers in Environmental Science*, *8*, 50. https://doi.org/10.3389/fenvs.2020.00050

Kögel-Knabner, I. & Rumpel, C. (2018). Advances in Molecular Approaches for Understanding Soil Organic Matter Composition, Origin, and Turnover: A Historical Overview. *Advances in Agronomy*, *Soil Biol. Biochem. 40 2008*, 1–48. https://doi.org/10.1016/bs.agron.2018.01.003

Kuzyakov, Y., Friedel, J. K. & Stahr, K. (2000). Review of mechanisms and quantification of priming effects. *Soil Biology and Biochemistry*, *32*(11–12), 1485–1498. https://doi.org/10.1016/s0038-0717(00)00084-5

Lal, R. (2004). Soil Carbon Sequestration Impacts on Global Climate Change and Food Security. *Science*, *304*(5677), 1623–1627. https://doi.org/10.1126/science.1097396

Lavallee, J. M., Soong, J. L. & Cotrufo, M. F. (2020). Conceptualizing soil organic matter into particulate and mineral-associated forms to address global change in the 21st century. *Global Change Biology*, *26*(1), 261–273. https://doi.org/10.1111/gcb.14859

Lehmann, J. & Kleber, M. (2015). The contentious nature of soil organic matter. *Nature*, *528*(7580), 60–68. https://doi.org/10.1038/nature16069

Leuthold, S. J., Haddix, M. L., Lavallee, J. & Cotrufo, M. F. (2023). Encyclopedia of Soils in the Environment (Second Edition). *Soil Analytical Chemistry*, 68–80. https://doi.org/10.1016/b978-0-12-822974-3.00067-7

Liyanage, L. R. M. C., Sulaiman, M. F., Ismail, R., Gunaratne, G. P., Dharmakeerthi, R. S., Rupasinghe, M. G. N., Mayakaduwa, A. P. & Hanafi, M. M. (2021). Carbon Mineralization Dynamics of Organic Materials and Their Usage in the Restoration of Degraded Tropical Tea-Growing Soil. *Agronomy*, *11*(6), 1191. https://doi.org/10.3390/agronomy11061191

Lloyd, J. & Taylor, J. A. (1994). On the Temperature Dependence of Soil Respiration. *Functional Ecology*, *8*(3), 315. https://doi.org/10.2307/2389824

Lützow, M. von, Kögel-Knabner, I., Ekschmitt, K., Flessa, H., Guggenberger, G., Matzner, E. & Marschner, B. (2007). SOM fractionation methods: Relevance to functional pools and to stabilization mechanisms. *Soil Biology and Biochemistry*, *39*(9), 2183–2207. https://doi.org/10.1016/j.soilbio.2007.03.007

Mirabito, A. J. & Chambers, L. G. (2023a). Quantifying mineral-associated organic matter in wetlands as an indicator of the degree of soil carbon protection. *Geoderma*, *430*, 116327. https://doi.org/10.1016/j.geoderma.2023.116327

Mirabito, A. J. & Chambers, L. G. (2023b). Quantifying mineral-associated organic matter in wetlands as an indicator of the degree of soil carbon protection. *Geoderma*, *430*, 116327. https://doi.org/10.1016/j.geoderma.2023.116327

Moyano, F. E., Manzoni, S. & Chenu, C. (2013). Responses of soil heterotrophic respiration to moisture availability: An exploration of processes and models. *Soil Biology and Biochemistry*, *59*, 72–85. https://doi.org/10.1016/j.soilbio.2013.01.002

Neve, S. D. & Hofman, G. (2002). Quantifying soil water effects on nitrogen mineralization from soil organic matter and from fresh crop residues. *Biology and Fertility of Soils*, *35*(5), 379–386. https://doi.org/10.1007/s00374-002-0483-3

Nissan, A., Alcolombri, U., Peleg, N., Galili, N., Jimenez-Martinez, J., Molnar, P. & Holzner, M. (2023). Global warming accelerates soil heterotrophic respiration. *Nature Communications*, *14*(1), 3452. https://doi.org/10.1038/s41467-023-38981-w

Olson, J. S. (1963). Energy Storage and the Balance of Producers and Decomposers in Ecological Systems. *Ecology*, *44*(2), 322–331. https://doi.org/10.2307/1932179

Paul, E. A. (2016). The nature and dynamics of soil organic matter: Plant inputs, microbial transformations, and organic matter stabilization. *Soil Biology and Biochemistry*, *98*, 109–126. https://doi.org/10.1016/j.soilbio.2016.04.001

Poeplau, C., Don, A., Six, J., Kaiser, M., Benbi, D., Chenu, C., Cotrufo, M. F., Derrien, D., Gioacchini, P., Grand, S., Gregorich, E., Griepentrog, M., Gunina, A., Haddix, M., Kuzyakov, Y., Kühnel, A., Macdonald, L. M., Soong, J., Trigalet, S., … Nieder, R. (2018). Isolating organic carbon fractions with varying turnover rates in temperate agricultural soils – A comprehensive method comparison. *Soil Biology and Biochemistry*, *125*, 10–26. https://doi.org/10.1016/j.soilbio.2018.06.025

Raza, T., Qadir, M. F., Khan, K. S., Eash, N. S., Yousuf, M., Chatterjee, S., Manzoor, R., Rehman, S. ur & Oetting, J. N. (2023). Unrevealing the potential of microbes in decomposition of organic matter and release of carbon in the ecosystem. *Journal of Environmental Management*, *344*, 118529. https://doi.org/10.1016/j.jenvman.2023.118529

Ren, B., Chen, P., Shaaban, M., Yang, X., Chen, Y., Zhang, Z., Chen, B., Peng, T. & Núñez-Delgado, A. (2022). Appraisal of different land use systems for heterotrophic respiration in a Karst landscape. *Environmental Research*, *212*(Pt C), 113480. https://doi.org/10.1016/j.envres.2022.113480

Rocci, K. S., Lavallee, J. M., Stewart, C. E. & Cotrufo, M. F. (2021). Soil organic carbon response to global environmental change depends on its distribution between mineral-associated and particulate organic matter: A meta-analysis. *Science of The Total Environment*, *793*, 148569. https://doi.org/10.1016/j.scitotenv.2021.148569

Sanderman, J. & Amundson, R. (2014). *Treatise on Geochemistry (Second Edition)*. 217–272. https://doi.org/10.1016/b978-0-08-095975-7.00807-x

Sawada, K., Funakawa, S. & Kosaki, T. (2016). Short-term respiration responses to drying–rewetting in soils from different climatic and land use conditions. *Applied Soil Ecology*, *103*, 13–21. https://doi.org/10.1016/j.apsoil.2016.02.010

Schmidt, M. W. I., Torn, M. S., Abiven, S., Dittmar, T., Guggenberger, G., Janssens, I. A., Kleber, M., Kögel-Knabner, I., Lehmann, J., Manning, D. A. C., Nannipieri, P., Rasse, D. P., Weiner, S. & Trumbore, S. E. (2011). Persistence of soil organic matter as an ecosystem property. *Nature*, *478*(7367), 49–56. https://doi.org/10.1038/nature10386

Shi, B., Hu, G., Henry, H. A. L., Stover, H. J., Sun, W., Xu, W., Wang, C., Fu, X. & Liu, Z. (2020). Temporal changes in the spatial variability of soil respiration in a meadow steppe: The role of abiotic and biotic factors. *Agricultural and Forest Meteorology*, *287*, 107958. https://doi.org/10.1016/j.agrformet.2020.107958

Six, J., Conant, R. T., Paul, E. A. & Paustian, K. (2002). Stabilization mechanisms of soil organic matter: Implications for C-saturation of soils. *Plant and Soil*, *241*(2), 155–176. https://doi.org/10.1023/a:1016125726789

Sleutel, S., Neve, S. D., Roibás, M. R. P. & Hofman, G. (2005). The influence of model type and incubation time on the estimation of stable organic carbon in organic materials. *European Journal of Soil Science*, *56*(4), 505–514. https://doi.org/10.1111/j.1365-2389.2004.00685.x

Sleutel, Steven, Moeskops, B., Huybrechts, W., Vandenbossche, A., Salomez, J., Bolle, S. D., Buchan, D. & Neve, S. D. (2008). Modeling Soil Moisture Effects on Net Nitrogen Mineralization in Loamy Wetland Soils. *Wetlands*, *28*(3), 724–734. https://doi.org/10.1672/07-105.1

Song, X., Zhu, J., He, N., Huang, J., Tian, J., Zhao, X., Liu, Y. & Wang, C. (2017). Asynchronous pulse responses of soil carbon and nitrogen mineralization to rewetting events at a short-term: Regulation by microbes. *Scientific Reports*, *7*(1), 7492. https://doi.org/10.1038/s41598-017-07744-1

Springob, G. & Kirchmann, H. (2003). Bulk soil C to N ratio as a simple measure of net N mineralization from stabilized soil organic matter in sandy arable soils. *Soil Biology and Biochemistry*, *35*(4), 629–632. https://doi.org/10.1016/s0038-0717(03)00052-x

Stockmann, U., Adams, M. A., Crawford, J. W., Field, D. J., Henakaarchchi, N., Jenkins, M., Minasny, B., McBratney, A. B., Courcelles, V. de R. de, Singh, K., Wheeler, I., Abbott, L., Angers, D. A., Baldock, J., Bird, M., Brookes, P. C., Chenu, C., Jastrow, J. D., Lal, R., … Zimmermann, M. (2013). The knowns, known unknowns and unknowns of sequestration of soil organic carbon. *Agriculture, Ecosystems & Environment*, *164*, 80–99. https://doi.org/10.1016/j.agee.2012.10.001

Tang, X., Du, J., Shi, Y., Lei, N., Chen, G., Cao, L. & Pei, X. (2020). Global patterns of soil heterotrophic respiration – A meta-analysis of available dataset. *CATENA*, *191*, 104574. https://doi.org/10.1016/j.catena.2020.104574

Védère, C., Lebrun, M., Honvault, N., Aubertin, M.-L., Girardin, C., Garnier, P., Dignac, M.-F., Houben, D. & Rumpel, C. (2022). How does soil water status influence the fate of soil organic matter? A review of processes across scales. *Earth-Science Reviews*, *234*, 104214. https://doi.org/10.1016/j.earscirev.2022.104214

Wang, J., Epstein, H. E. & Wang, L. (2010). Soil CO2 flux and its controls during secondary succession. *Journal of Geophysical Research: Biogeosciences*, *115*(G2), n/a-n/a. https://doi.org/10.1029/2009jg001084

Wang, Z.-Y., Xie, J.-B., Wang, Y.-G. & Li, Y. (2020). Biotic and Abiotic Contribution to Diurnal Soil CO2 Fluxes from Saline/Alkaline Soils. *Scientific Reports*, *10*(1), 5396. https://doi.org/10.1038/s41598-020-62209-2

Yan, Z., Bond-Lamberty, B., Todd-Brown, K. E., Bailey, V. L., Li, S., Liu, C. & Liu, C. (2018). A moisture function of soil heterotrophic respiration that incorporates microscale processes. *Nature Communications*, *9*(1), 2562. https://doi.org/10.1038/s41467-018-04971-6

Yang, S., Jansen, B., Absalah, S., Kalbitz, K., Castro, F. O. C. & Cammeraat, E. L. H. (2022). Soil organic carbon content and mineralization controlled by the composition, origin and molecular diversity of organic matter: A study in tropical alpine grasslands. *Soil and Tillage Research*, *215*, 105203. https://doi.org/10.1016/j.still.2021.105203

Yu, W., Huang, W., Weintraub-Leff, S. R. & Hall, S. J. (2022). Where and why do particulate organic matter (POM) and mineral-associated organic matter (MAOM) differ among diverse soils? *Soil Biology and Biochemistry*, *172*, 108756. https://doi.org/10.1016/j.soilbio.2022.108756

8. APPENDICES

APPENDIX A

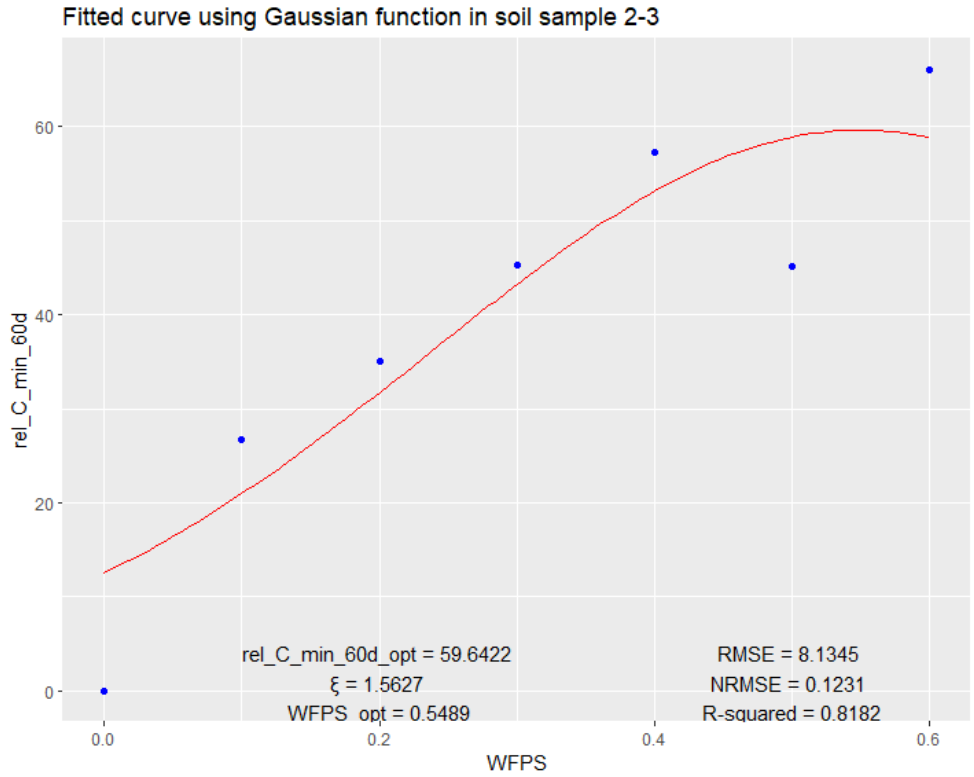

Fig. A.1 *Gaussian function fitting of relative cumulative C-mineralization with WFPS in soil samples 2-3*

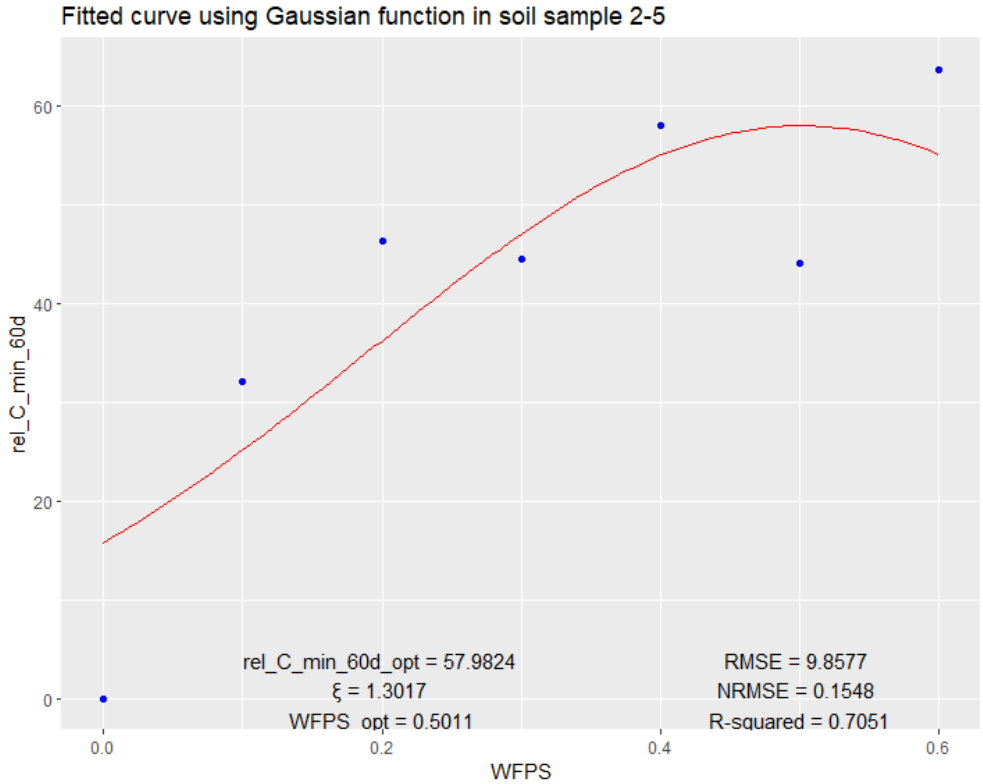

Fig. A.2 *Gaussian function fitting of relative cumulative C-mineralization with WFPS in soil samples 2-5*

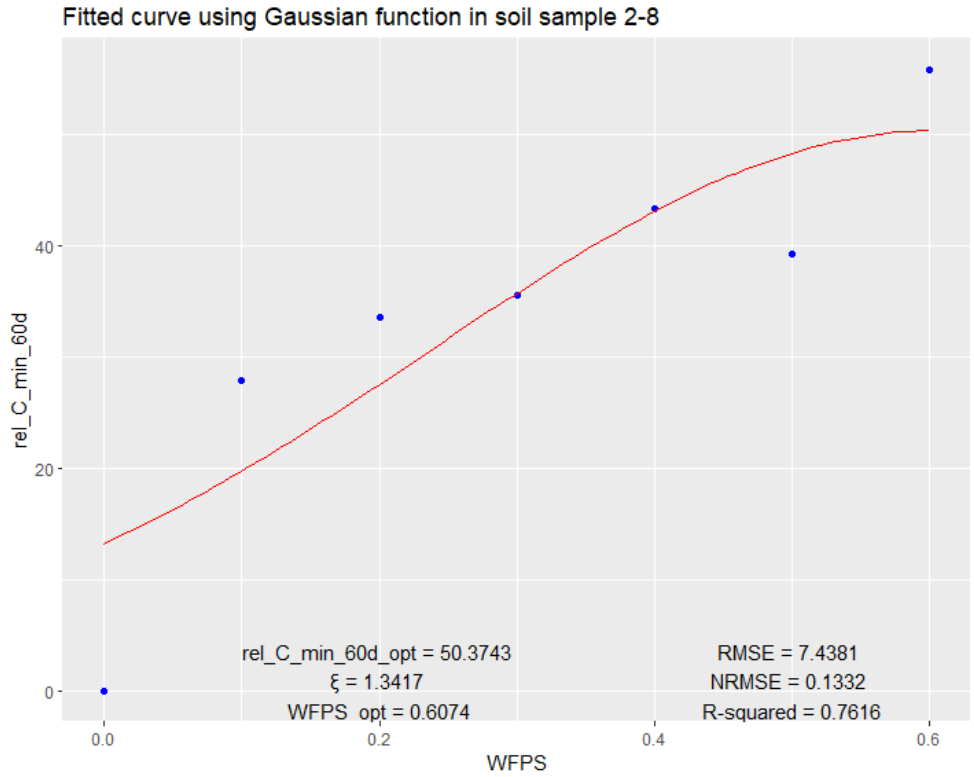

Fig. A.3 *Gaussian function fitting of relative cumulative C-mineralization with WFPS in soil samples 2-8*

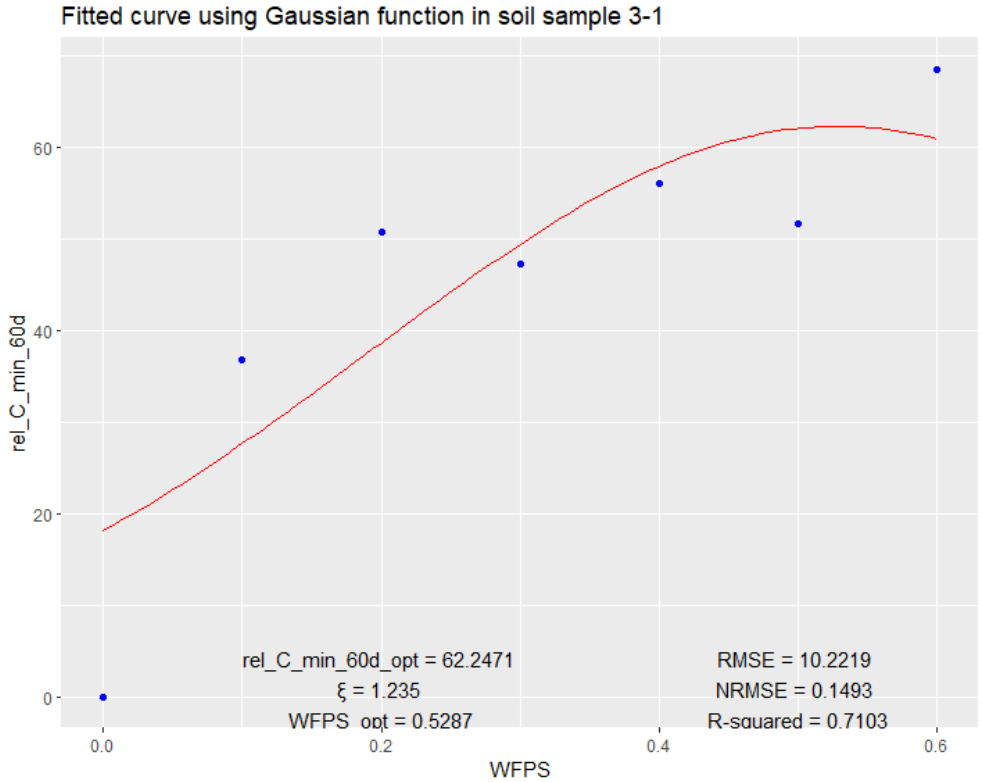

Fig. A.4 *Gaussian function fitting of relative cumulative C-mineralization with WFPS in soil samples 3-1*

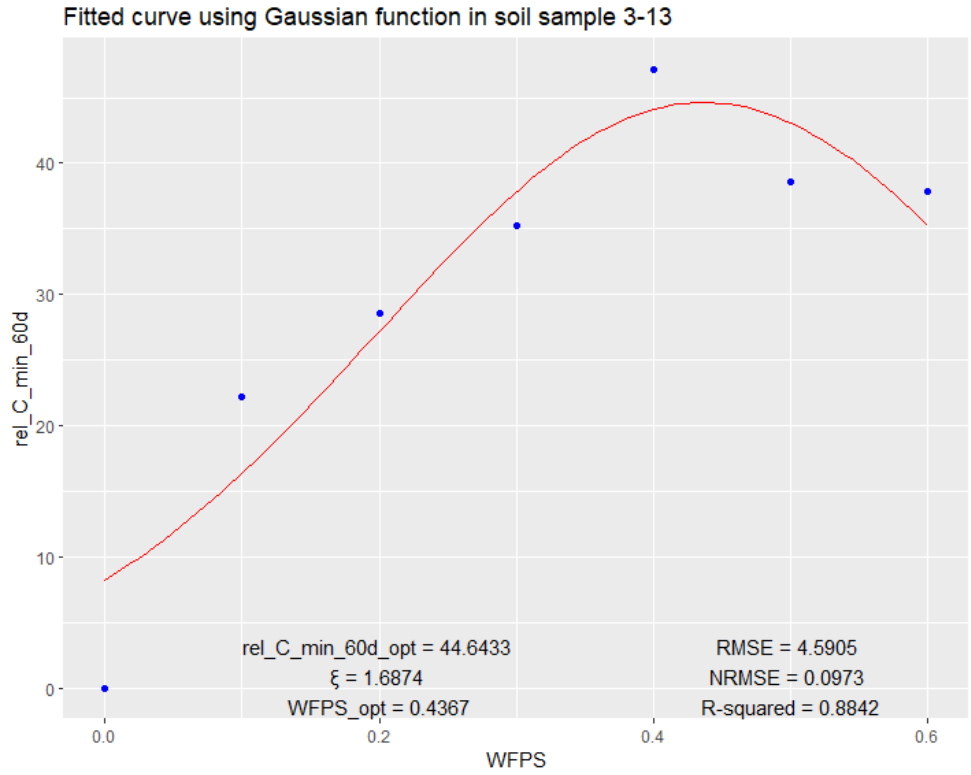

Fig. A.5 *Gaussian function fitting of relative cumulative C-mineralization with WFPS in soil samples 3-13*

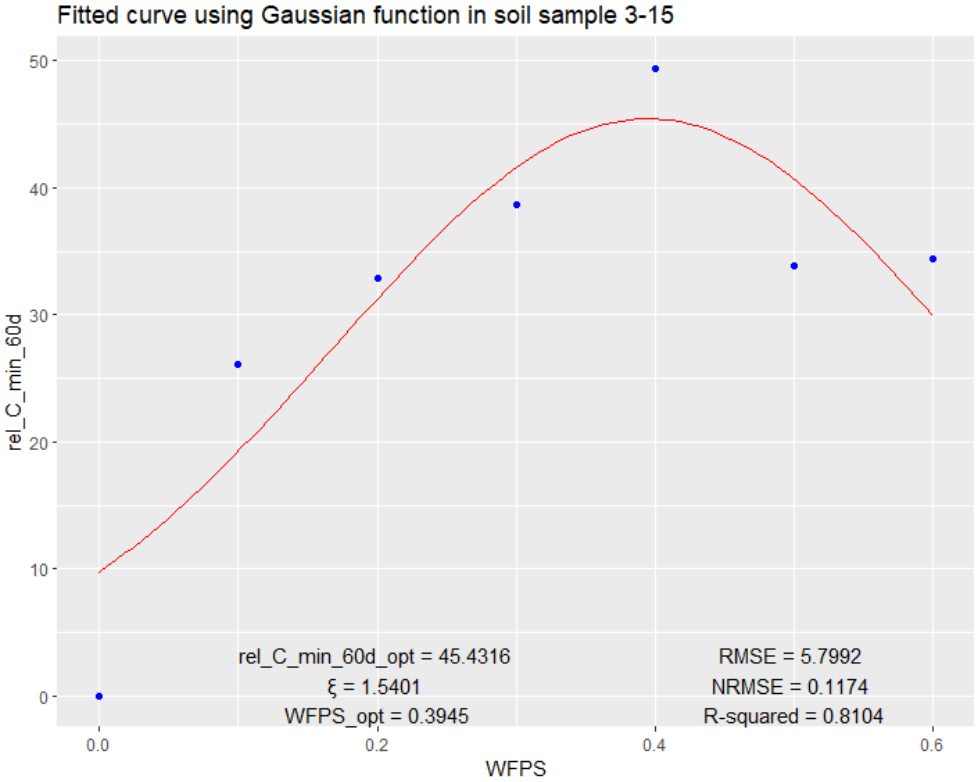

Fig. A.6 *Gaussian function fitting of relative cumulative C-mineralization with WFPS in soil samples 3-15*

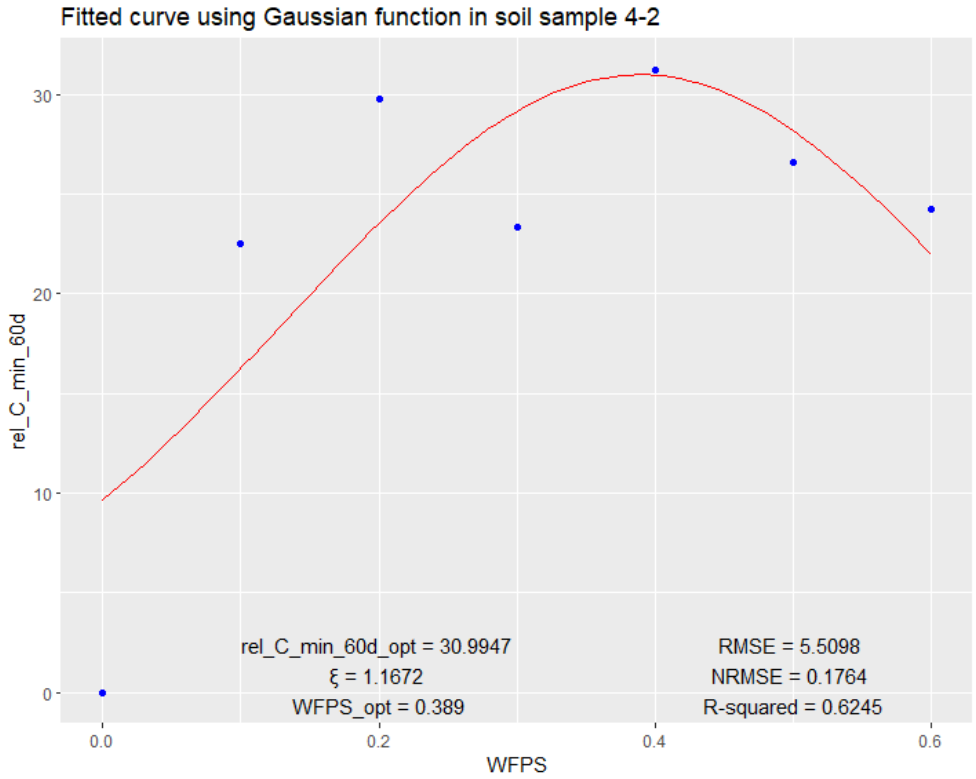

Fig. A.7 *Gaussian function fitting of relative cumulative C-mineralization with WFPS in soil samples 4-2*

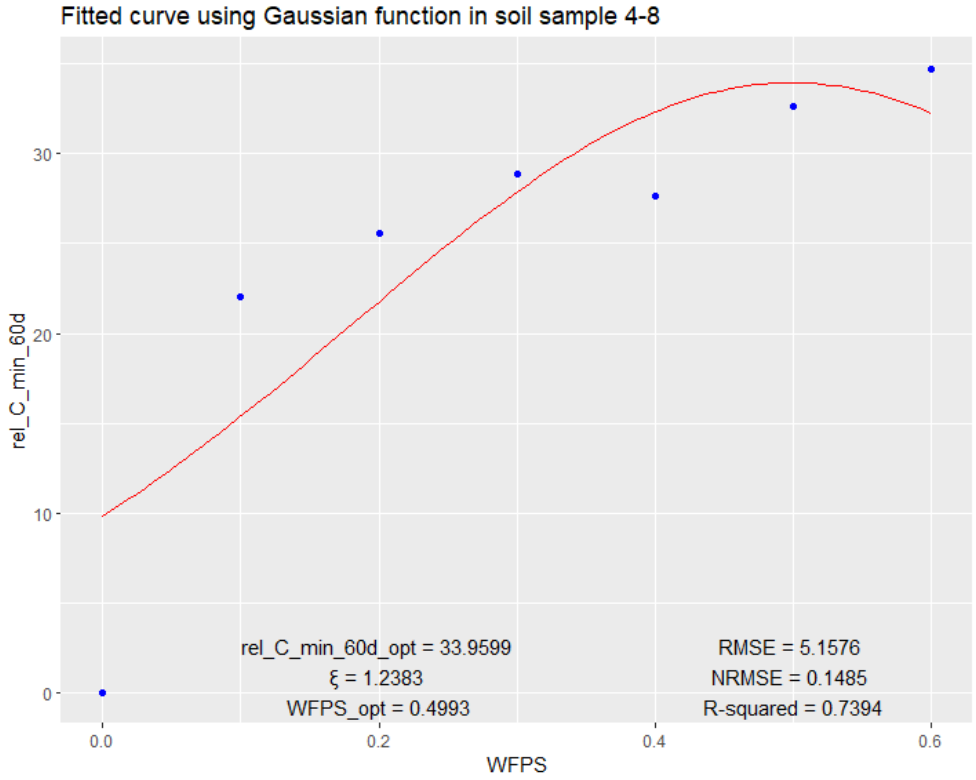

Fig. A.8 *Gaussian function fitting of relative cumulative C-mineralization with WFPS in soil samples 4-8*

APPENDIX B

***Table B**: Soil tube information across different moisture levels in the experiment (10%, 30%, 50%, and 20%, 40%, 60%)*

Soil tube information at different moisture levels (10%, 30%, 50%)		
Tube number	Soil sample number	WFPS
R1	1-4	10%
R2	1-4	10%
R3	2-3	10%
R4	2-3	10%
R5	2-5	10%
R6	2-5	10%
R7	2-8	10%
R8	2-8	10%
R9	3-1	10%
R10	3-1	10%
R11	1-4	30%
R12	1-4	30%
R13	2-3	30%
R14	2-3	30%
R15	2-5	30%
R16	2-5	30%
R17	2-8	30%
R18	2-8	30%
R19	3-1	30%
R20	3-1	30%
R21	1-4	50%
R22	1-4	50%
R23	2-3	50%
R24	2-3	50%
R25	2-5	50%
R26	2-5	50%
R27	2-8	50%
R28	2-8	50%
R29	3-1	50%
R30	3-1	50%
B1	3-13	10%
B2	3-13	10%
B3	3-15	10%
B4	3-15	10%
B5	4-2	10%
B6	4-2	10%
B7	4-5	10%
B8	4-5	10%
B9	4-8	10%
B10	4-8	10%
B11	3-13	30%
B12	3-13	30%
B13	3-15	30%
B14	3-15	30%
B15	4-2	30%
B16	4-2	30%
B17	4-5	30%
B18	4-5	30%
B19	4-8	30%
B20	4-8	30%
B21	3-13	50%
B22	3-13	50%
B23	3-15	50%
B24	3-15	50%
B25	4-2	50%
B26	4-2	50%
B27	4-5	50%
B28	4-5	50%
B29	4-8	50%
B30	4-8	50%

Soil tube information at different moisture levels (20%, 40%, 60%)		
Tube number	Soil sample number	WFPS
R1	1-4	20%
R2	1-4	20%
R3	2-3	20%
R4	2-3	20%
R5	2-5	20%
R6	2-5	20%
R7	2-8	20%
R8	2-8	20%
R9	3-1	20%
R10	3-1	20%
R11	1-4	40%
R12	1-4	40%
R13	2-3	40%
R14	2-3	40%
R15	2-5	40%
R16	2-5	40%
R17	2-8	40%
R18	2-8	40%
R19	3-1	40%
R20	3-1	40%
R21	1-4	60%
R22	1-4	60%
R23	2-3	60%
R24	2-3	60%
R25	2-5	60%
R26	2-5	60%
R27	2-8	60%
R28	2-8	60%
R29	3-1	60%
R30	3-1	60%
B1	3-13	20%
B2	3-13	20%
B3	3-15	20%
B4	3-15	20%
B5	4-2	20%
B6	4-2	20%
B7	4-5	20%
B8	4-5	20%
B9	4-8	20%
B10	4-8	20%
B11	3-13	40%
B12	3-13	40%
B13	3-15	40%
B14	3-15	40%
B15	4-2	40%
B16	4-2	40%
B17	4-5	40%
B18	4-5	40%
B19	4-8	40%
B20	4-8	40%
B21	3-13	60%
B22	3-13	60%
B23	3-15	60%
B24	3-15	60%
B25	4-2	60%
B26	4-2	60%
B27	4-5	60%
B28	4-5	60%
B29	4-8	60%
B30	4-8	60%

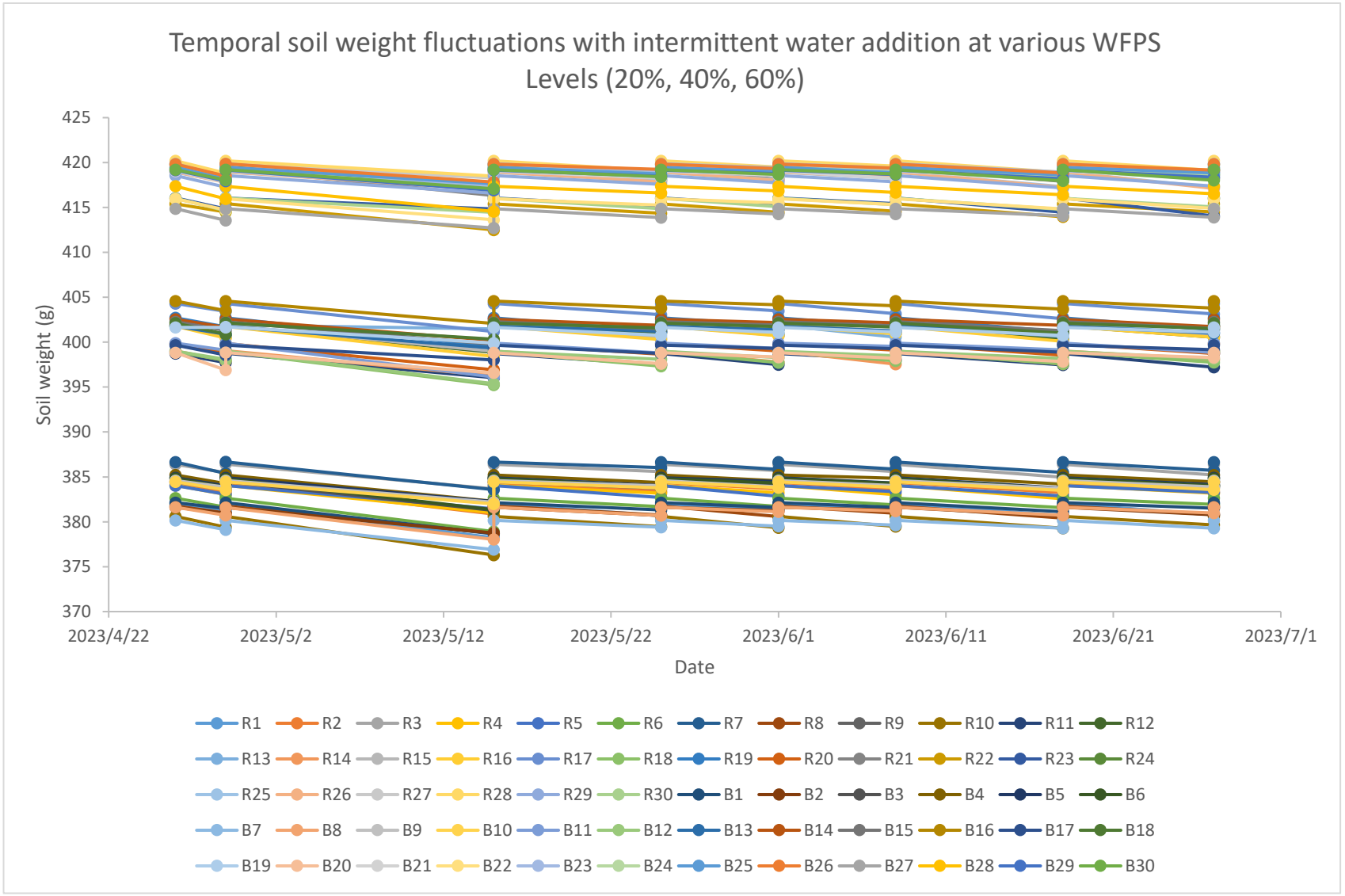

Fig. B 1 *Temporal soil weight changes with intermittent water addition for maintaining target WFPS levels (20%, 40%, 60%)*

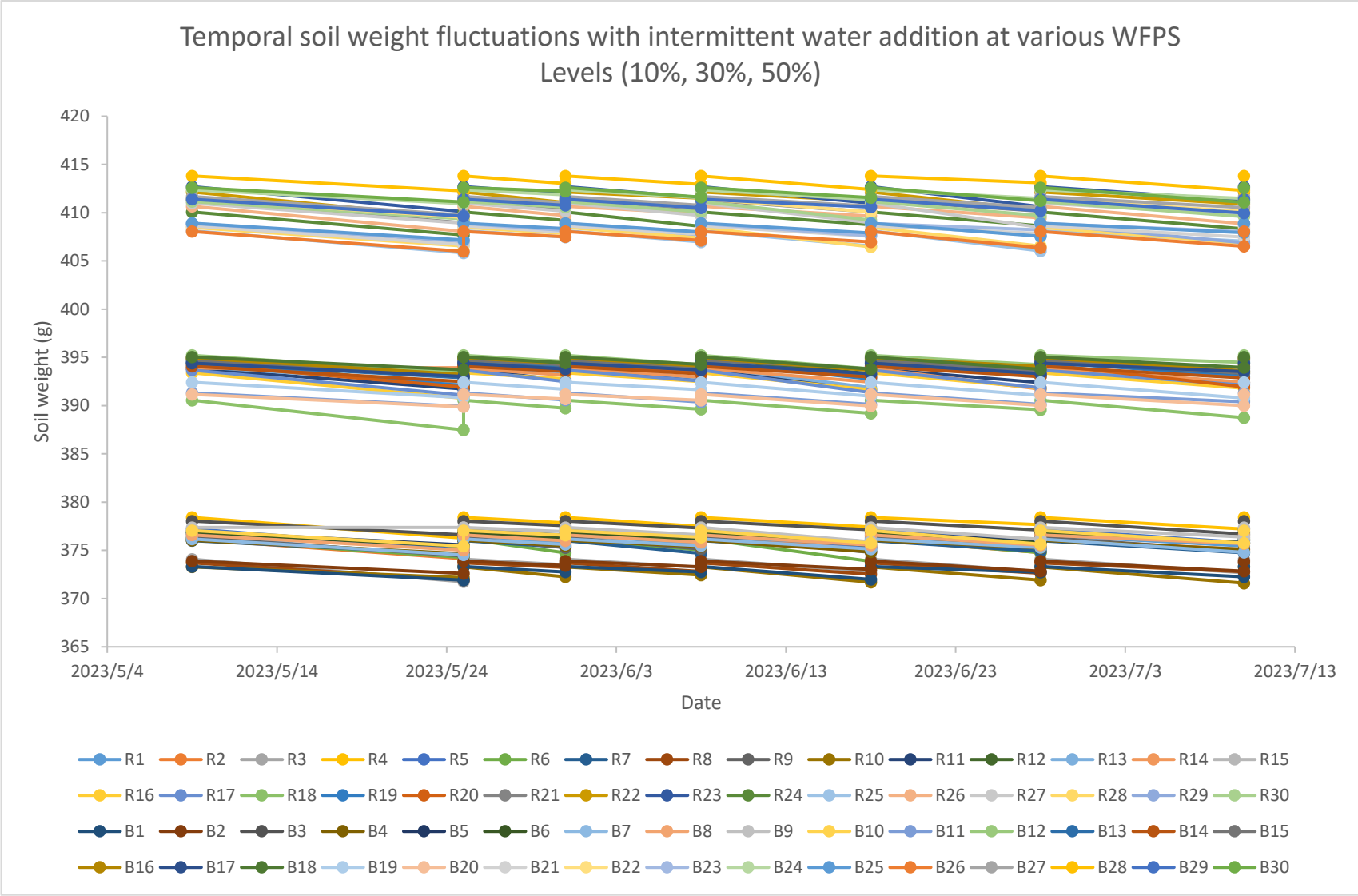

Fig. B 2 *Temporal soil weight changes with intermittent water addition for maintaining target WFPS levels (10%, 30%, 50%)*